EFFECTS OF MARATHON TRAINING ON MALE AND FEMALE FEMORAL STRESS FRACTURE RISK

A Thesis

presented to

the Faculty of California Polytechnic State University,

San Luis Obispo

In Partial Fulfillment

of the Requirements for the Degree

Master of Science in Biomedical Engineering

by

Clara Lin

November 2020

COMMITTEE MEMBERSHIP

TITLE: Effects of Marathon Training on Male and Female Femoral Stress Fracture Risk

AUTHOR: Clara Lin

DATE SUBMITTED: November 2020

COMMITTEE CHAIR: Scott Hazelwood, Ph.D.
Professor of Biomedical Engineering

COMMITTEE MEMBER: Michael Whitt, Ph.D.
Professor of Biomedical Engineering

COMMITTEE MEMBER: Kristen O'Halloran Cardinal, Ph.D.
Professor of Biomedical Engineering

ABSTRACT

Effects of Marathon Training on Male and Female Femoral Stress Fracture Risk

Clara Lin

Marathon runners are prone to femoral stress fractures due to the high magnitudes and frequencies of lower extremity loads during training. Female runners tend to have a greater incidence of stress fracture compared to male runners. Sex-specific differences in body structure, joint pressure, and muscle activation patterns that influence bone remodeling may cause this observed difference in stress fracture occurrence. The goal of this thesis was to develop a finite element model of the femur during marathon training, then determine if marathon training affected bone properties of male and female runners differently. To achieve this goal, a finite element femur model was integrated with a bone remodeling algorithm. Sex-specific muscle and joint pressure loads corresponding to baseline activity and marathon training were applied to the finite element femur model. Axial strain, density, damage, and remodeling activity were quantified at regions predicted to be at high risk of stress fracture. The major results of this analysis predicted that marathon training increased bone damage at all regions of interest in both males and females, especially at the inferior neck. The model predicted that the superior neck, trochanter, and proximal diaphysis were more severely weakened in females than males after marathon training. While this model cannot directly quantify femoral stress fracture risk, it may be used to predict regions of bone weakness in male and female marathon

runners. Future work may be done to improve accuracy of this model by using sex-specific femur geometry and bone remodeling parameters specific to male and female marathon runners. This model may be useful in future applications to study effectiveness of injury preventive methods, such as gait retraining, in reducing bone damage.

Keywords: Stress fracture, marathon running, bone remodeling, finite element

ACKNOWLEDGMENTS

Thank you to my advisor Dr. Scott Hazelwood for his valuable guidance and support throughout the research process.

Additionally, thank you to my professors, family, and friends who have provided support and encouragement throughout my studies.

TABLE OF CONTENTS

Page

LIST OF TABLES

Table Page

LIST OF FIGURES

Figure Page

Chapter 1
INTRODUCTION

1.1 Motivation

Marathon racing is becoming more popular with a 49% increase in participants worldwide between 2008 to 2018 [1]. This increase is partially attributed to the growing participation of women in the sport. As the popularity of marathon racing increases, so does the prevalence of running-related injuries. Running a marathon is equivalent to taking approximately 25,000 steps with ground reaction forces three to five times body weight, and internal forces up to ten times body weight [2]. Due to this high volume of repetitive loading, lower extremity stress fractures comprise 30% of injuries among distance runners [3].

Stress fractures are bone injuries that reflect a mismatch between bone strength and mechanical load. Unlike acute fractures caused by a single traumatic event in which bone is loaded above its maximum strength, stress fractures develop when loads below the maximum bone strength are applied over many cycles. Stress fractures result from bone fatigue and insufficient bone toughness [4]. Fatigue failure occurs when localized damage accumulates in healthy bone over many loading cycles and coalesces into a fracture. Insufficiently tough bone typically has lower bone mineral density, so the remaining bone tissue must bear more load and is at a higher risk of fracture from loading during normal activities. Both bone fatigue and insufficient bone toughness are attributed to microcracks in bone tissue. Bone experiences high loads from muscle contractions. During loading, bone tissue is elastically deformed until it reaches a point of irreversible plastic deformation in the form of

a microcrack [4]. Microcracks reduce bone toughness and resistance to fracture. Bone toughness depends on the critical stress intensity factor, which is determined by microdamage accumulation prior to crack development and the energy required for crack propagation [5]. Unlike other materials which fail under fatigue, bone has a biological remodeling response to repair itself. Microcracks are normally repaired through bone remodeling, but accumulation of microcracks can propagate into a stress fracture if they are not repaired fast enough. The microcrack repairing process also temporarily reduces bone's density and load-bearing ability as damaged bone is resorbed. Development of microcracks is expected in healthy bone due to normal loading, but microcrack accumulation is evidence of bone fatigue combined with an imbalance between removal of damaged bone and creation of new bone. A large accumulation of microcracks indicates that the bone tissue does not have sufficient time to remodel, adapt to the loading conditions, and repair damage [4]. Stress fractures can develop as a result of excessive microdamage accumulation and bone remodeling.

Bone is a living tissue that adapts to its mechanical and biological environment through remodeling. Bone remodels in response to load and damage. Increased loading leads to increased bone mass, while decreased loading leads to decreased bone mass. Presence of microcracks initiates bone remodeling to replace damaged bone with new bone. Damage is the primary stimulus for bone remodeling in runners. Bone remodeling occurs in five phases: activation, resorption, reversal, formation, and quiescence. Osteoclasts are bone cells responsible for resorption, and osteoblasts are bone cells responsible for

formation. Osteocytes are bone cells that are believed to detect a mechanical stimulus or damage to activate the remodeling response. Figure 1.1 shows the cells involved in the bone remodeling process. Osteoclasts absorb bone tissue at the remodeling site and leave behind a resorption cavity. This temporary cavity increases bone porosity and weakness during the reversal phase. During formation, osteoblasts fill the resorption cavity with osteoid, or unmineralized bone. Finally, mineralization of the new bone begins during the quiescence phase. This process of resorbing and refilling takes 3-4 months at each remodeling site [6].

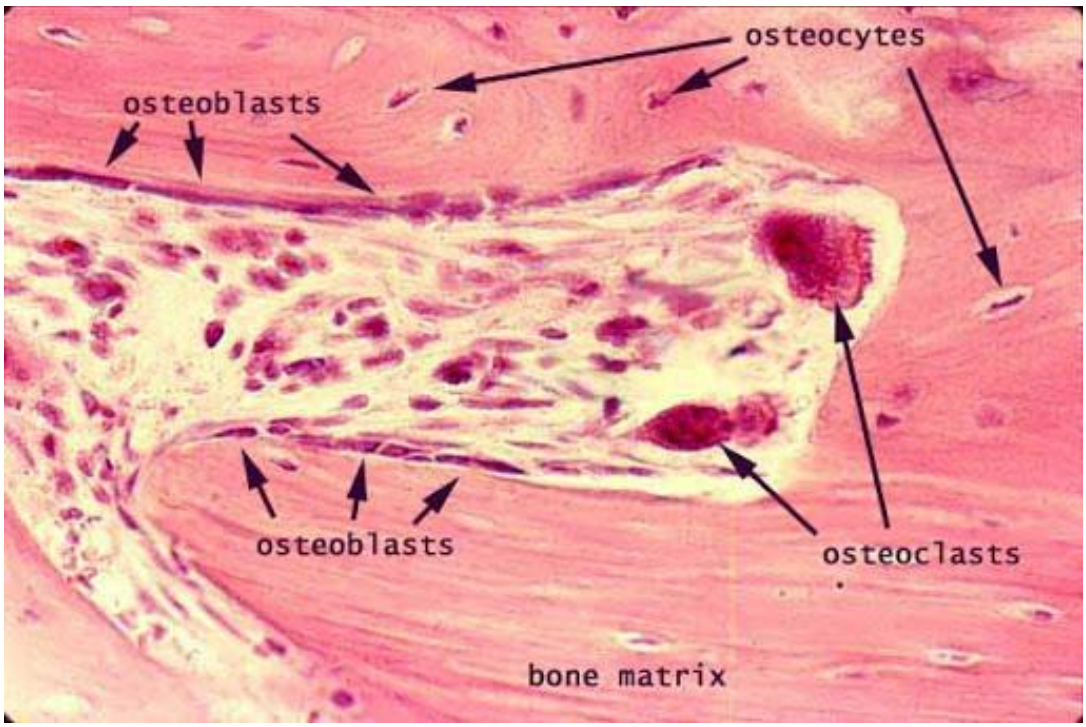

Figure 1.1 Bone remodeling cells [7]

The time lag between resorption and formation leads to increased fracture risk if load is continuously applied. When appropriate rest is taken, remodeling can remove damage and strengthen bone. On the other hand, a lack of rest time and continued loading on weak bone can lead to a positive feedback cycle of more strain, microdamage, and bone resorption [8]. When osteoclastic activity outweighs osteoblastic activity, the bone is at high risk of stress fracture. Runners who increase training intensity or mileage experience a greater amount of fatigue microdamage that the remodeling response may not repair fast enough. Even if remodeling activation increases in response to the greater microdamage, the remodeling process results in a temporarily weak state of bone before new bone formation and mineralization is complete. This paradox of bone remodeling preventing yet promoting stress fracture affects distance runners whose bones consistently experience high magnitude and frequency of loading.

The most commonly reported locations of stress fractures in runners include the tibia, femur, and fibula [3], [4]. Femoral fractures are especially difficult to treat and diagnose. The most common symptom of a femoral stress fracture is hip or groin pain during exercise, which prompts diagnosis by radiograph or MRI imaging [3]. The recovery time for a conservative femoral neck stress fracture ranges from eight to fourteen weeks, while more severe fractures may require up to a year before returning to activity [9]. Additionally, severe fractures often require surgical fixation and rehabilitation. Untreated femoral fractures may result in avascular necrosis of the femoral head

and require total hip replacement [3], [9]. Therefore, understanding the mechanisms behind this injury and preventing fracture development is optimal.

Prior studies show that a discrepancy in stress fracture occurrence between male and female runners exists [10], [11], [12], but the reason has not been clearly identified. Potential causes include sex-specific trends in running kinematics and muscle activation patterns. Finite element modeling has been used to study strain's effect on bone adaptation, as well as peak load and fracture locations of bone. Stress fractures result from cyclic fatigue of bone, so developing a model that accounts for the high number of loading cycles associated with marathon training is important. Most finite element studies have focused on walking and falling, but not distance running [13]. Existing models of bone remodeling during distance running fail to account for sex-specific differences, creating a need for further research in this field. Understanding the effects of microdamage accumulation and bone remodeling in male and female runners may improve intervention methods to prevent stress fracture.

1.2 Prior Work

At present, little information exists on sex-based differences in bone remodeling and microdamage associated with marathon running. Female runners are twice as likely to sustain lower body injuries than males [14], but a gap in research of female-specific risk factors for injury exists. Variations in body structure [15]-[18], gait kinematics [18], [19], and muscle activation [20], [21] are theorized to contribute to the increased number of running injuries observed in females. Variations in hip geometry (Figure 1.2) may cause males and females to

run with different mechanics that contribute to different injuries over the course of many repetitions [18].

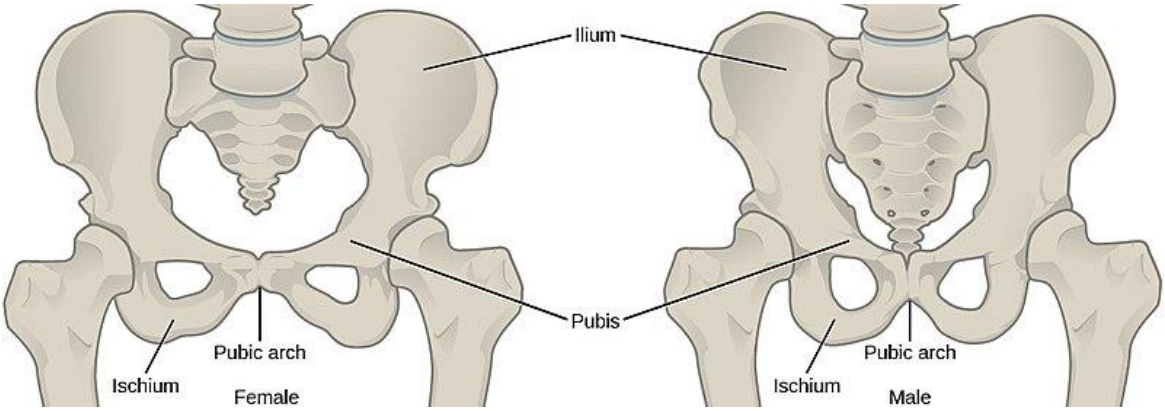

Figure 1.2 Differences in male and female hip geometry [22]

Prior studies by Iglic et al. [15] and Kralj-Iglič et al. [17] investigated the effects of male and female hip geometry on peak hip joint stress. Geometric parameters analyzed from hip radiographs included distance between medial acetabular rims, pelvis height and width, and angle from the femoral head center to lateral edge of the acetabulum [17]. These studies determined that females had a significantly smaller hip articular surface radius and larger distance between acetabular rims. Kralj-Iglič found that the average female femoral head radius was 0.3 cm shorter than the average male femoral head radius [17]. The effect of this small difference in femoral head radius is magnified by the resulting increase in hip joint stress. Hip joint stress is joint contact force divided by the hip articular surface area. A smaller femoral head radius entails less surface area

coverage of the femoral head in the acetabulum. This smaller load-bearing area creates a high contact stress on the hip cartilage and bone [17]. Normalized for effects of body weight, the smaller surface area in females contributes to a 20% higher hip joint contact pressure.

For their stature, females have a wider inter-hip distance compared to males [15]-[17]. This proportionally wider pelvis increases hip joint stress [16]-[18] and contributes to greater peak hip adduction observed in females [19]-[21]. A greater hip adduction angle is unfavorable because it places greater demands on the abductor muscles. Hip abductor muscles are responsible for stabilizing the femoral head in the acetabulum and stabilizing the pelvis horizontally during the single-leg stance of gait [23]. Females tend to experience greater pelvic obliquity, in which one hip is higher than the other, compared to males [24]. Pelvic obliquity may be caused by leg length inequality or contractures of connective tissue at the hip. Greater hip abductor muscle activation reduces this pelvic obliquity motion. Therefore, females may compensate for the mechanical disadvantage of body structure by increasing abductor muscle force production. Decreased efficiency of the abductor muscles can lead to early fatigue and greater loading on the bone. A wider inter-hip distance also increases the angle of the femur necessary to bring the knees together, which decreases mechanical efficiency [25]. This angular tilt on the hips and knees increases stress on these bones [20]. As seen by higher hip joint stress and increased demand of the abductor muscles, differences in hip geometry are more biomechanically unfavorable for females.

Male and female runners are observed to have different muscle activation patterns. Prior studies found that females activate their gluteal muscles more than males while running [18], [21]. Gluteal muscle activity is significant because increased activation correlates with higher joint stress and risk of developing running injuries. Electromyography (EMG) studies have analyzed muscle activation patterns during running. EMG data depends on conduction velocities and muscle unit activation potentials associated with different muscle fiber cross-sectional areas and fiber types. A study by Willson et al. [21] collected lower extremity kinematic and gluteal muscle activation data for male and female runners. Females ran with 53% greater average gluteus maximus activation compared to males. This difference in muscle activation can contribute to earlier muscle fatigue, altered running kinematics, and injury. Chumanov et al. [18] placed EMG surface electrodes on leg muscles to collect muscle activation data from runners on a treadmill. The EMG signals were then processed and reported as integrated muscle activity across the entire gait cycle. This study found similarly that female gluteus maximus activity was twice that of males [18]. Females also exhibited higher gluteus medius and vastus lateralis activation that increased with running speed and running surface inclination. Changes in muscle activation have been shown to alter the distribution of bone strain, so bone may experience high loads in areas where it has not been adapted to do so [26]. These observed differences in muscle activation patterns during running may contribute to greater fracture risk in females.

A study by Sinclair [19] examined three-dimensional kinematics and kinetics of male and female runners to determine susceptibility of females to overuse injuries. Females had significantly greater knee abduction, knee internal rotation, and ankle eversion. No significant kinetic differences in impact parameters of tibial acceleration and ground reaction force between sexes were observed. This study concluded that the greater risk of females developing stress fractures is due to the bone remodeling response to mechanical stress, and not just load impact. The key takeaway from this study is that consideration of bone remodeling is critical when analyzing causes for stress fracture. The current knowledge of sex-specific differences in running loads applied to a bone remodeling model can provide more information on the discrepancy in stress fractures between male and female runners.

Prior studies have focused on bone remodeling and computational modeling of the femur under various loading conditions [27], [28]. Stress fractures result from an imbalance in bone remodeling with greater damage formed than removed. Bone remodeling is a dynamic biological process that renews the skeleton to adapt to mechanical loads. The mechanistic bone remodeling algorithm by Hazelwood et al. assumes that low load levels on bone or presence of fatigue microdamage activates remodeling [6]. Loading is proportional to the strain range from daily activities and number of cycles performed per day for each activity. Remodeling removes bone when this mechanical loading falls below a threshold. In the case of marathon running, remodeling is activated to replace damaged tissue. Bone experiences high

repetitive loads during running that trigger microcrack development. The remodeling response activates in the presence of microcracks to replace the weak and damaged bone with new bone. Basic multicellular units (BMUs) are groups of cells responsible for the remodeling process. Osteoclasts resorb bone and leave behind resorption cavities refilled by osteoblasts. Remodeling has the potential to strengthen bone by repairing damaged bone tissue, but also the potential to weaken bone as the number of resorption cavities increases. More resorption cavities can lead to greater porosity and weaker load bearing ability. Loading during running influences BMU activation frequency, bone density, and microdamage. Remodeling plays a critical role in the skeleton's response to distance running and risk of stress fracture.

Quantifying bone remodeling and damage through clinical studies are inconvenient and invasive, so computational models are an optimal way to study bone’s dynamic processes. Prior studies have used computational models to analyze bone mineral density and regions of stress fracture but have not investigated male and female running cases [27]. There is a gap in research on the differences in bone remodeling that occur in male and female runners, as well as how these differences relate to stress fracture rates. A two-dimensional finite element femur model developed by Hazelwood and Castillo [27] simulated bone remodeling during beginner, intermediate, and advanced marathon training schedules. This study determined that marathon training caused BMU remodeling activity to increase above baseline values in the cortical regions of the neck and proximal cortex. Microdamage observed after marathon training

was greater than baseline values at all locations measured. This prior model can be improved upon by expanding the two-dimensional joint and abductor muscle loads to three-dimensional femur geometry and specific muscle loads. A prior study by Deuel [28] developed a three-dimensional femur finite element model to study remodeling under walking and stair-climbing loads with different types of hip implants. The model uses a load profile for a hip replacement patient during walking and stair-climbing. Deuel's three-dimensional model can be modified to simulate male and female marathon running. Table 1.1 below provides a summary of the prior work discussed in Section 1.2.

Table 1.1 Summary of prior work

Iglic et al. [15], Kralj-Iglic et al. [17]	Differences in female hip geometry & hip joint stress: • Wider pelvis • Smaller hip articular surface • Higher hip joint stress
Willson et al. [21], Chumanov et al. [18]	Differences in female muscle activation while running: • Higher gluteus maximus, gluteus medius, vastus lateralis activation
Sinclair [19]	Differences in female running kinematics: • Greater knee abduction, knee internal rotation, ankle eversion
Hazelwood et al. [6]	Mechanistic bone remodeling algorithm
Hazelwood and Castillo [27]	2D finite element femur model of bone remodeling during marathon training
Deuel [28]	3D finite element femur model of bone remodeling with different hip implants

1.3 Objectives

The objective of this thesis is to investigate strain, bone density, remodeling activation, and microdamage at common femoral stress fracture sites in males and females following marathon training. Analyzing differences in these bone properties can provide a better understanding of the etiology behind the higher incidence of femoral stress fractures observed in females.

These bone properties will be assessed from a three-dimensional femur finite element model integrated with a bone remodeling algorithm. Initial baseline values for porosity, damage, and activation frequency will be established by applying loading conditions simulating daily activity until steady state values representative of a mature adult femur are achieved. The model will be validated against data from an experimental study of cadaveric femora. Once validated, the model will then simulate male and female runners during a sixteen-week marathon training regimen. Any differences in bone properties can then be compared across the baseline and running models for each sex.

This study seeks to answer whether differences in male and female femoral loading during marathon training have a significant effect on strain, bone density, remodeling activation, and microdamage that correspond to stress fracture. Marathon training is predicted to decrease bone strength for both males and females. Female runners are hypothesized to exhibit lower bone density, higher remodeling activation, and more microdamage at sites of interest after

marathon training, which may contribute to the greater incidence of stress fractures compared to males.

Chapter 2

METHODS

2.1 Finite Element Model Development

The finite element model used in this study was based on a three-dimensional femur model developed by Deuel [28]. The distal portion of the femur and the condyles were excluded in this model because this portion does not have a significant effect on the strains in the proximal regions of interest. The development of the finite element model as described in Section 2.1, including the meshing of the geometry, was performed by Deuel [28] and subsequently used for the analysis described in this thesis. The femur model was created from a CT scan of a male cadaveric femur with soft tissue removed. Next, Mimics software converted the femur CT scan into an initial two-dimensional triangular surface mesh. This surface mesh was then converted into a three-dimensional mesh of quadratic tetrahedral elements using Patran software. Prior work by Viceconti et al. determined that quadratic tetrahedral elements were the best choice to model a solid femur [29]. The localized coordinate system consisted of the z-axis aligned with the longitudinal axis of the femur. The femur was rigidly fixed at the distal end. The initial model consisted of homogeneous material properties representative of cortical bone with a Poisson's ratio of 0.3.

This model already underwent a convergence study and had an appropriate mesh density. Deuel [28] performed a convergence study using five different meshes with increasing number of elements to select the appropriate mesh density. The convergence study applied hip joint contact and abductor

forces to the five models with different meshes, then compared principle strains and displacements for convergence. The final mesh selected consisted of 29,175 elements and 41,723 nodes. This convergence study was determined appropriate for the scope of this study, so the same mesh was used. Finite element analyses were performed using Abaqus (Dassault Systems, Waltham, MA).

2.1.1 Bone Remodeling Algorithm

The bone remodeling algorithm developed by Hazelwood et al. [6] was incorporated into this finite element model through an Abaqus user subroutine. This mechanistic model accounts for the effects of biological processes such as remodeling space porosity and lag time on bone remodeling. The algorithm simulates bone adaptation by the bone remodeling process responding to low levels of loading on bone and fatigue microdamage. A mechanical stimulus, ϕ, is determined as being proportional to strain, s, from different activities and the number of cycles per day each activity was performed, R_L (Equation 1). The stress exponent parameter, q, was set to 4 [30]. When stimulus values fall below an equilibrium stimulus, bone is considered to be insufficiently loaded. The equilibrium stimulus for this model was estimated to be $\phi_0 = 1.88 \times 10^{10}$ cycles per day [6]. Fatigue microdamage occurs in proportion to the stimulus applied, leading to an increase in the rates of bone remodeling.

$$\phi = \sum_{i=1}^{n} s_i^q R_{Li} \qquad \text{(Equation 1)}$$

The algorithm assumes bone to be linear elastic with an evolving elastic modulus, E, dependent on porosity, p, given by Equation 2a for cortical bone and

Equation 2b for trabecular bone. Cortical and trabecular bone have different elastic moduli due to differences in bone architecture. Cortical bone, characterized by its compact and lamellar microstructure, is defined as having a bone mineral density above 1.8 g/cm^3 in this model. Trabecular bone is composed of rod-shaped trabeculae that create high surface exposure to bone marrow and blood flow. Trabecular bone is defined in this model as having bone mineral density below 1.8 g/cm^3. Elastic modulus, measured in units of MPa in this model, quantifies the stiffness of bone tissue and its resistance to elastic deformation under applied load. Nine variables (porosity, minimum principle strain for each step, damage potential, equilibrium damage, number of refilling BMUs, number of resorbing BMUs, and activation frequency) are updated at each time step. Porosity, equilibrium damage, and activation frequency are variables of interest in this study. Porosity is the void volume per unit volume of bone. Porosity and elastic modulus change with internal remodeling in response to load levels and damage. Osteoclasts create remodeling spaces with the removal of bone, which increases bone porosity and weakens bone structure. Apparent density, ρ, is defined as the wet mineralized bone tissue mass per volume of bone tissue [31]. The assumed relationship between apparent density and porosity is inversely linear, so elastic modulus can be calculated from porosity. Conversion of porosity to apparent density is based on the following determined by experimental data [6], [31]: density = 2g/cm^3 for a porosity of 0, density = 0g/cm^3 for a porosity of 1 (Equation 3). This relationship is applied to both cortical and trabecular bone. The change in porosity is assumed to be a function of activation frequency history. The rate of fatigue damage accretion

is the difference in fatigue damage formation and removal rates, which are affected by bone resorption and refilling rates for each BMU. Bone resorption and refilling rates are based on an average osteon cement line diameter of 0.190 mm, a 24-day resorption period, and a 64-day formation period. Activation frequency is a function of load levels and the existing state of damage on the internal surface area of a bone region. Activation frequency measures the rate of bone remodeling by number of new BMUs created per unit area of bone tissue per day and is reported in units of BMUs/mm^2/day. Activation frequency is distinct from bone formation rate, which is the volume of bone produced per unit of time. Damage is the total crack length per section area of bone (mm/mm^2).

for $p < 0.097$:

$$E_{cortical}(in\ MPa) = 23440(1-p)^{5.74} \qquad \text{(Equation 2a)}$$

for $p \geq 0.097$:

$$E_{trabecular}(in\ MPa) = 14927(1-p)^{1.33} \qquad \text{(Equation 2b)}$$

$$\rho = 2(1-p) \qquad \text{(Equation 3)}$$

2.1.2 Joint and Muscle Forces

Hip joint contact and muscle forces for the single leg stance phase of walking and stair climbing were applied to the model to establish baseline bone material properties for an individual performing everyday activities. These loads represent the heel-strike and toe-off phases of normal walking and maximum forces experienced during stair climbing. Gluteus medius, gluteus minimus, adductor longus, adductor brevis, psoas, vastus lateralis, and vastus medialis muscle groups were represented [28]. Muscle loads were applied to selected nodes based on anatomical attachment areas. Magnitudes and directions of these forces for a 725 N (163 lbf.) male and 556 N (125 lbf.) female were derived from the work of McLeish and Charnley [32]. These body weights are representative of typical male and female marathon runners [33], [34]. The locations and magnitudes of the muscle and hip joint contact loads are shown below in Figure 2.1 for baseline heel-strike, toe-off, and stair climbing load cases. This image is representative of the loading conditions for a baseline male femur. Adjustments in hip joint and abductor muscle load magnitude, as well as abductor load angle, were later incorporated in the female model.

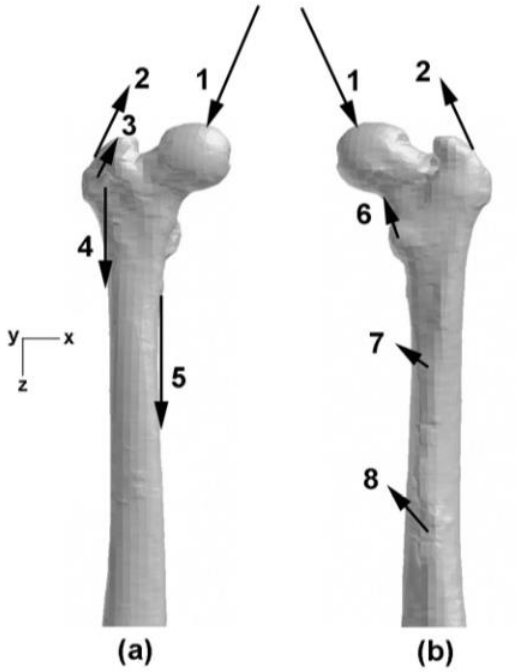

Force	*Force Magnitude at Load Case (% body weight)*		
	I	**II**	**III**
1. Hip joint	250	250	270
2. Gluteus medius	84	84	101
3. Gluteus minimus	41	40	40
4. Vastus lateralis	76	-	101
5. Vastus medialis	-	-	202
6. Psoas	-	19	-
7. Adductor brevis	10	10	10
8. Adductor longus	23	23	23

Figure 2.1 (a) Anterior and (b) posterior view of baseline hip contact and muscle forces applied to the femur model as a percentage of body weight for loading case I (heel-strike), case II (toe-off), and case III (stair climbing). (Image from Deuel [28])

Abductor muscle (gluteus medius, gluteus minimus) angles were adjusted to model the structural differences between male and female hips. Hip joint forces are dependent on the ratio of body weight moment arm to abductor muscle moment arm [35]. In this study, the abductor muscle moment arm is

defined as the distance from the insertion point of the gluteus medius on the greater trochanter to the center of the hip joint. Figure 2.2 below shows the locations of these forces and moment arms at the hip joint. Females have a shorter abductor muscle moment arm than males [36]. A decrease in the abductor muscle moment arm leads to an increase in abductor muscle force necessary for gait. Females also have a larger body weight moment arm due to their wider pelvis. These physiological differences were modeled by calculating the abductor load angle in the x-z plane. The direction of the hip contact load was assumed to be the same for males and females since prior studies found no significant difference between angles at the femoral neck [16]. The loads for each condition are summarized below in Table 2.1 for males and Table 2.2 for females with respect to the coordinate system in Figure 2.3. Appendix A contains the detailed calculation.

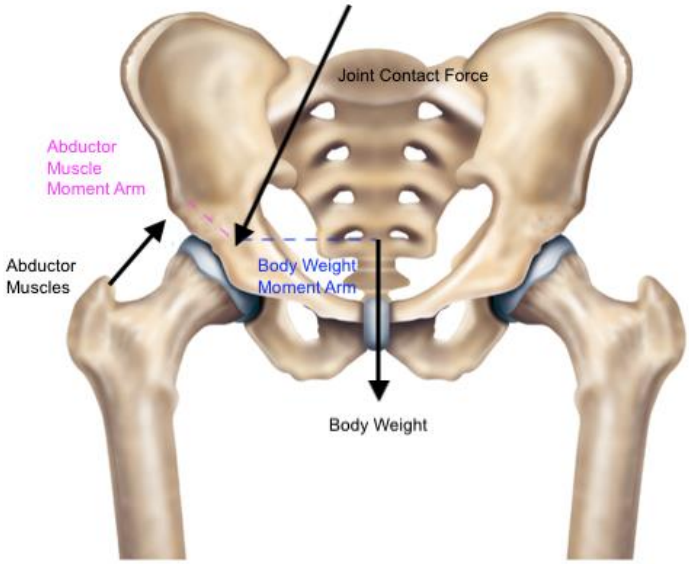

Figure 2.2 Locations of abductor muscle and body weight moment arm at the hip [35]

Females tend to experience greater joint pressure due to a smaller average hip articular surface radius [16], [17]. For an equally massive male and female, the female is expected to have greater peak hip joint stress. This difference in bone structure was simulated by increasing the joint pressure based on peak stress normalized to body weight ratios found by Iglic et al. [15]. Iglic et al. found that female hip joint stress was 26% higher than males when normalized to body weight. The baseline hip joint stress while walking was set to 3.33 MPa for a 725 N male and 3.20 MPa for a 556 N female. The detailed calculation is shown in Appendix B.

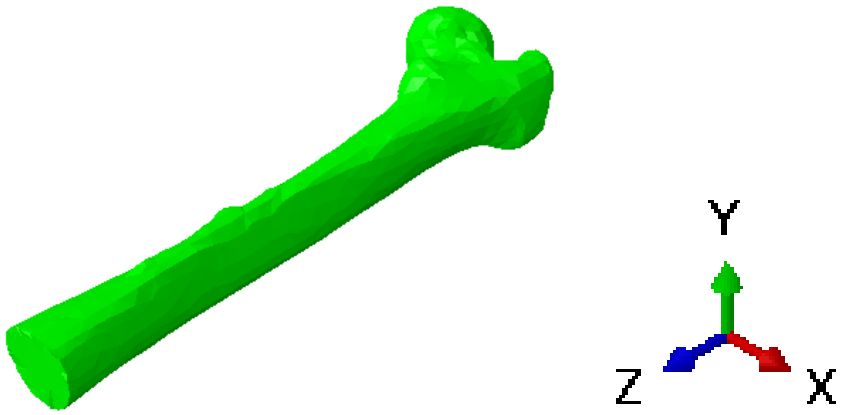

Figure 2.3 Femur in coordinate system

Table 2.1 Finite element loads for a 725 N body weight male

	Magnitude [N]	x-z angle [deg]	y-z angle [deg]
	HEEL-STRIKE		
Gluteus Medius	607	-24	-31
Gluteus Minimus	300	-24	-31
Vastus Lateralis	550	0	9
Adductor Brevis	73	-53	9
Adductor Longus	167	-45	14
Joint Pressure [MPa]	3.33	-22	31
	TOE-OFF		
Gluteus Medius	611	-24	9
Gluteus Minimus	289	-24	9
Psoas	136	-18	-34
Adductor Brevis	73	-53	9
Adductor Longus	167	-45	14
Joint Pressure [MPa]	3.33	-21	-9
	STAIRCLIMBING		
Gluteus Medius	731	-24	-45
Gluteus Minimus	290	-24	-45
Vastus Lateralis	732	0	9
Vastus Medialis	1468	0	9
Adductor Brevis	73	-53	9
Adductor Longus	167	-45	14
Joint Pressure [MPa]	3.43	-21	45
	RUNNING		
Gluteus Medius	1092	-24	-31
Gluteus Minimus	540	-24	-31
Vastus Lateralis	550	0	9
Adductor Brevis	73	-53	9
Adductor Longus	167	-45	14
Joint Pressure [MPa]	6.99	-22	31

Table 2.2 Finite element loads for a 556 N body weight female

	Magnitude [N]	x-z angle [deg]	y-z angle [deg]
	HEEL-STRIKE		
Gluteus Medius	465	-19.4	-31
Gluteus Minimus	230	-19.4	-31
Vastus Lateralis	422	0	9
Adductor Brevis	56	-53	9
Adductor Longus	128	-45	14
Joint Pressure [MPa]	3.2	-22	31
	TOE-OFF		
Gluteus Medius	468	-19.4	9
Gluteus Minimus	289	-19.4	9
Psoas	104	-18	-34
Adductor Brevis	56	-53	9
Adductor Longus	128	-45	14
Joint Pressure [MPa]	3.2	-21	-9
	STAIRCLIMBING		
Gluteus Medius	561	-19.4	-45
Gluteus Minimus	223	-19.4	-45
Vastus Lateralis	562	0	9
Vastus Medialis	1126	0	9
Adductor Brevis	56	-53	9
Adductor Longus	128	-45	14
Joint Pressure [MPa]	3.3	-21	45
	RUNNING		
Gluteus Medius	1117	-19.4	-31
Gluteus Minimus	414	-19.4	-31
Vastus Lateralis	527	0	9
Adductor Brevis	56	-53	9
Adductor Longus	128	-45	14
Joint Pressure [MPa]	6.72	-22	31

2.2 Model Validation

Model validation consisted of comparing axial strain values from the finite element model to experimental strain values found by Deuel [38]. Deuel loaded three pairs of cadaveric femora to simulate the single-leg stance phase of walking for native, resurfacing hip implant, and tapered femoral stem implant conditions. Data from the native femur was used to validate this finite element model. Strain gages measured bone surface strains at four locations: proximomedial, proximolateral, distomedial, and distolateral. A custom-made fixture attached to an Instron Material Testing Machine applied a joint contact force to the femoral head and an abductor muscle force to the greater trochanter. A 1000 lb. load cell between the acetabular cup and test fixture measured the joint contact force. A turnbuckle and steel cable attached to the greater trochanter created the abductor muscle force.

The male and female baseline models were established by running the remodeling simulation for 730 iterations to achieve steady state values of porosity, damage, and activation frequency. Steady state was defined as changes in porosity less than 0.5%, and changes in damage and activation frequency less than 5% over 30 iterations [28]. Then, an additional force step was applied to model Deuel's experimental loading conditions [28], [38]. A 1100 N load applied to the femoral head 22° from the z-axis in the x-z plane simulated the joint contact force. A 555 N load applied to the greater trochanter 27° from the z-axis in the x-z plane simulated the abductor load. The locations of these loads can be seen in Figure 2.1 in Section 2.1.2. The abductor load corresponds

to gluteus medius and minimus muscle forces. Axial strains for four elements were averaged in approximate regions of the strain gage locations in Deuel's experiment [38]. Comparing these strains to the experimental surface strains found by Deuel validated the finite element model.

2.3 Marathon Loading Conditions

To simulate marathon training, the model incorporated muscle and joint loads specific to male and female runners (Tables 2.1 and 2.2). First, the baseline walking loads were scaled based on values found in prior studies of lower extremity loads experienced during running. These running loads were then adjusted for females, as described in Section 2.1.2 and calculated in Appendices A and B. The direction of the loads during running were modeled to be in heel-strike because prior studies have found that peak hip joint contact force occurs during the first 0-30% of the gait cycle [13], [39].

Joint contact force while running increases to 5.2 times body weight, compared to 2.5 times body weight while walking [40]. For the male subject, the joint contact pressure increased proportionally from 3.33 MPa during walking to 6.99 MPa during running. The female joint contact pressure increased from 3.20 MPa during walking to 6.72 MPa during running. The magnitudes of the abductor muscle forces increased proportionally by the same scale factor. These muscles are significant because gluteal muscles produce the most substantial increase in force production out of other hip muscles while running [41].

Prior studies have found that females exhibit higher gluteus maximus, gluteus medius and vastus lateralis muscle activation while running [18], [21].

Chumanov et al. collected electromyographic data at the gluteus medius and vastus lateralis of males and females running at various speed and incline conditions [18]. Based on the results of this study, the female gluteus medius load was increased by a scale factor of 1.33 and the vastus lateralis load was increased by a scale factor of 1.25 for the analysis in this thesis.

The bone remodeling code was modified to vary the loading rate depending on day of the training schedule [42]. The simulated marathon training cycle (Appendix C) was 16 weeks long and concluded with a 26-mile marathon. The program consisted of running 0-20 miles per day. Weekly mileage ranged from 28-45 miles with 2 rest days per week, for 598 miles total. This training program was designed for an intermediate level runner accustomed to running approximately 30 miles per week before starting marathon training. Daily running mileage was converted to cycles per day by assuming 85 cycles per minute at a 7.5 minute per mile pace [27]. The bone remodeling code was written in Fortran and integrated into the finite element model using an Abaqus user subroutine. Different marathon training schedules may be modeled by modifying the code to vary the number of rest days or mileage.

2.4 Solution Steps

The femur model was initially composed of homogeneous cortical bone material properties. Loading conditions representative of everyday activity were applied over 730 iterations until a steady state bone distribution was achieved. The three steps per day consisted of muscle and joint pressure loading patterns for heel-strike, toe-off, and stair-climbing. Heel-strike and toe-off were each

applied for 5,000 cycles per day, and stair-climbing was applied for 40 cycles per day. These values for cycles per day were determined based on data from healthy adults [43]. Repeating these three activities over 730 iterations established the baseline model representative of a skeletally mature adult femur. The 730 iterations needed to achieve steady state properties in the remodeling parameters was determined by Deuel [28]. The model achieved steady state when changes in porosity were less than or equal to 0.5%, and changes in damage and activation frequency were less than or equal to 5% over 30 iterations.

After achieving this baseline model of the femur, the sixteen-week marathon training schedule began. 5,000 cycles per day of heel-strike and toe-off loading conditions were applied to model daily activity, but the stair-climbing step was replaced with a step incorporating running loads to model marathon training. At the end of the sixteen-week training period, strain, porosity, activation frequency, and damage were analyzed at regions of interest.

2.5 Regions of Interest

Common locations for running-induced femoral stress fractures determined the regions of interest analyzed in this study. These regions include the superior neck, inferior neck, proximal diaphysis, and trochanter [13], [27], [44], [45]. These regions are shown on the finite element model in Figure 2.4. There has been little research on why femoral stress fractures commonly occur at these locations, but Edwards hypothesized that the combination of the small diameter of the femoral neck with large anterior and medial shear forces during

running contribute to a greater fracture risk [46]. Axial strain, density, remodeling activation, and microdamage in the selected regions of interest were measured before and after the 16-week marathon training plan. These values were quantified by taking the average over eight elements in each region of interest.

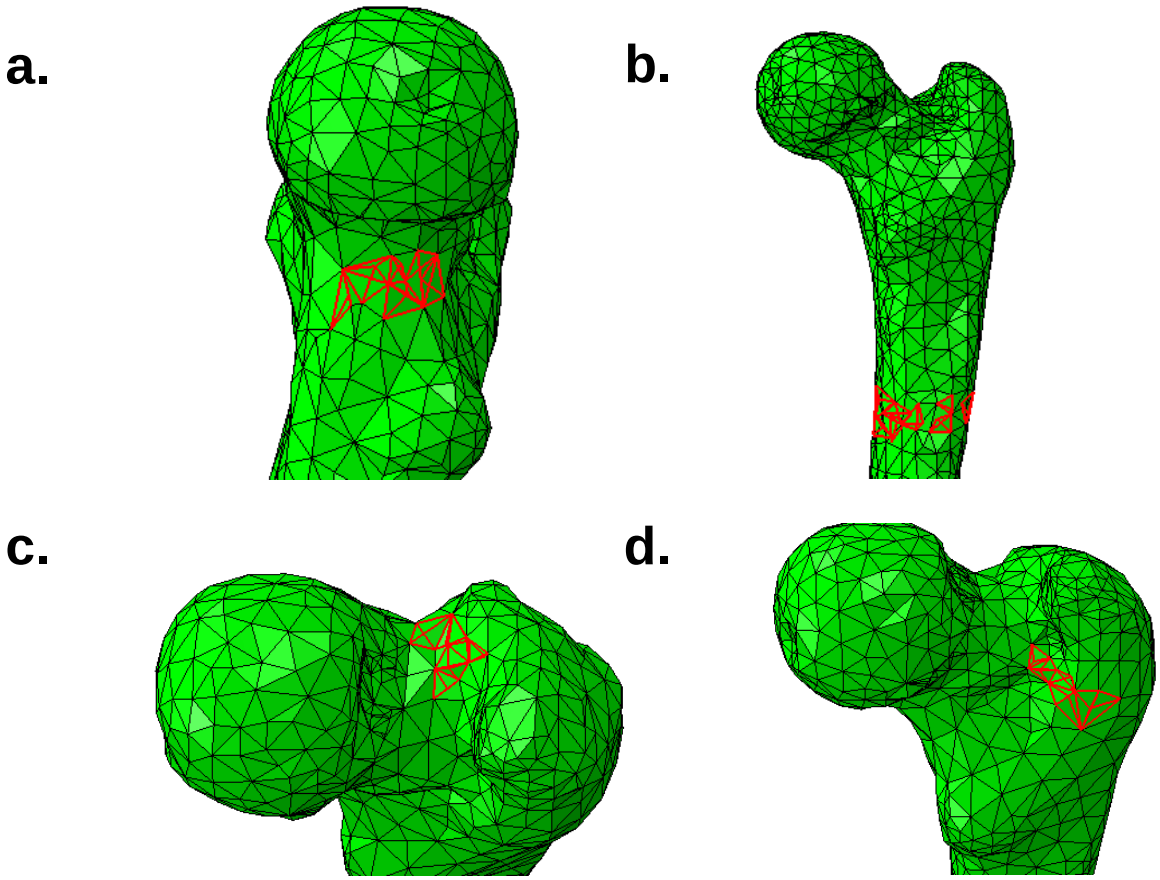

Figure 2.4 Regions of interest for stress fracture

(a) Inferior neck
(b) Proximal diaphysis
(c) Superior neck
(d) Intertrochanteric Region

Chapter 3

RESULTS

3.1 Model Validation

This model was validated by comparing average axial strain at four locations on the femur between the finite element model and the cadaveric femur experimental data collected by Deuel [38]. Figure 3.1 shows the four sites of axial strain measurement. Axial strain was measured in microstrain (Microstrain = Strain × 10^6). Validation results are listed in Table 3.1. Femur strain may vary greatly depending on subject body weight, bone shape, and bone stiffness. Based on high variability among subjects and acceptance criteria used in prior studies [28], an acceptance range of two standard deviations away from experimental results was determined appropriate for validation. The strains in the finite element model were within one standard deviation of the experimental results at the proximal medial, distal medial, and distal lateral locations. The strain at the proximal lateral region was slightly below one standard deviation of the experimental value. This discrepancy could have resulted from a lower male body weight (725 N) used in the FE-model compared to the body weight of the patient that the cadaveric femur belonged to. A typical hip arthroplasty patient weighs 836 N [47]. Therefore, this model was considered validated.

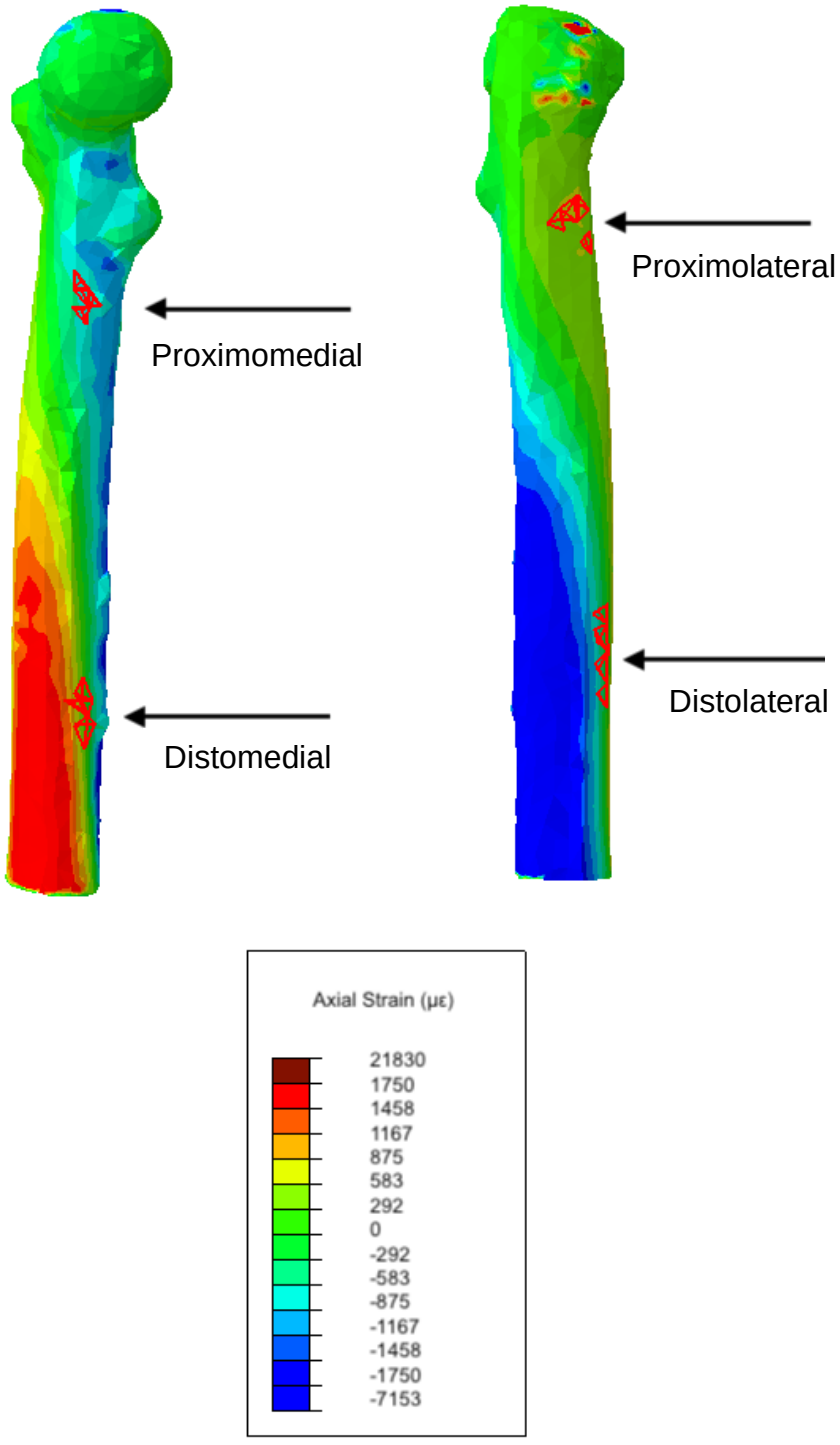

Figure 3.1 Locations and magnitudes of experimental strain measurements for model validation.

(Strain is measured in microstrain, Microstrain=Strain × 10^6)

Table 3.1 Comparison of experimental and FEA strain results for FEA model validation

Femoral Location	Experimental Strain Results from Deuel [38] (Mean ± Std. Dev.)	FEA Strain Results
Proximal Medial	-621 ± 96	-629
Proximal Lateral	637 ± 59	534
Distal Medial	40 ± 35	33
Distal Lateral	-126 ± 57	-130

*Strain is reported as microstrain (Microstrain = Strain × 10^6). Tensile strain is positive and compressive strain is negative.

3.2 Finite Element Analysis Results

The finite element model density results (Figure 3.2) matched clinically observed femoral bone density distributions [48]. Key features observed included a dense cortical bone shell around the diaphysis, porous medullary canal, and varying density at the femoral head and trochanter. The model predicted a 21-23% decrease in density at the inferior neck and a 4-6% decrease in density at the proximal diaphysis after completing sixteen weeks of marathon training (Figure 3.3). Males and females were predicted to have the greatest difference in bone density at the superior neck (Figure 3.4). Superior neck bone density was predicted lower for both the baseline and marathon training female models compared to the male models. Figure 3.5 displays baseline and marathon training bone mineral density results for males and females.

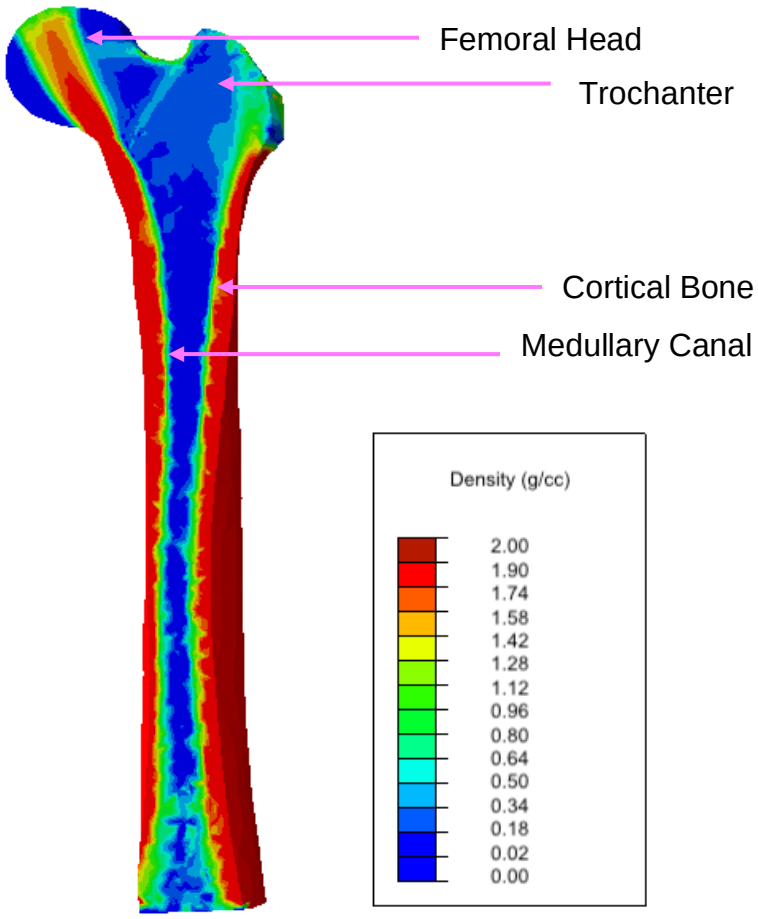

Figure 3.2 Density distribution of male baseline femur

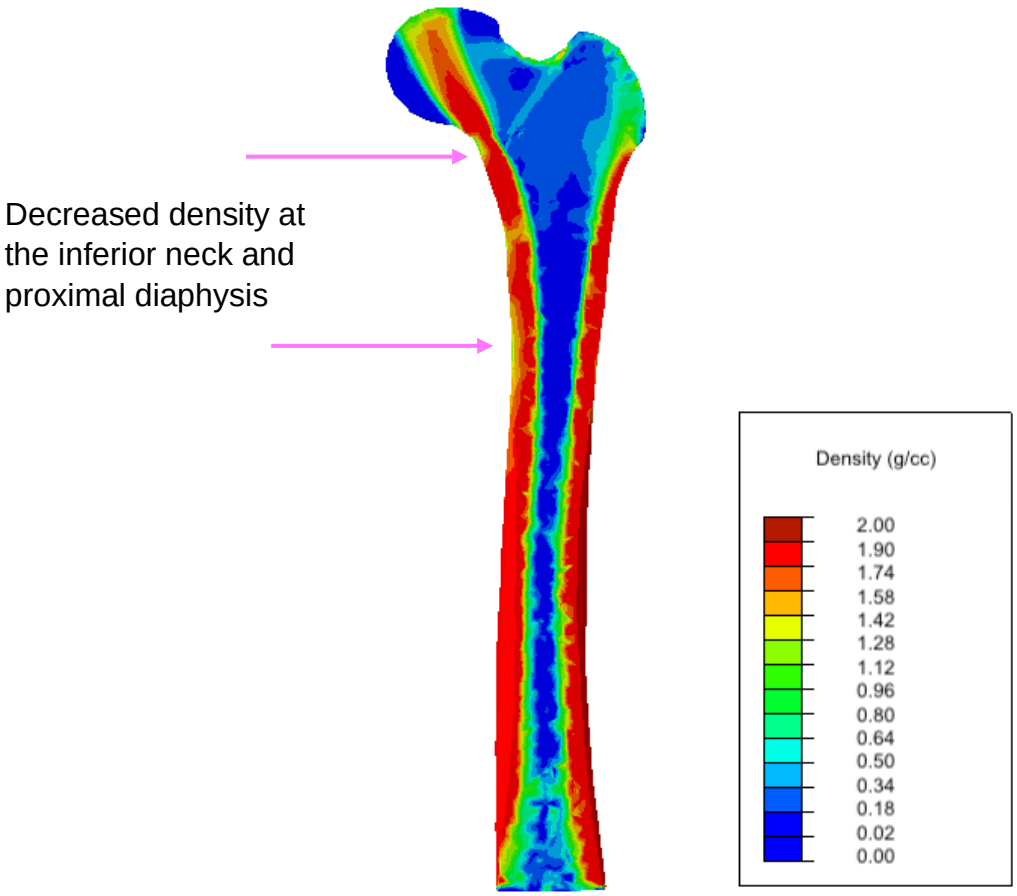

Figure 3.3 Density distribution of male femur after marathon training

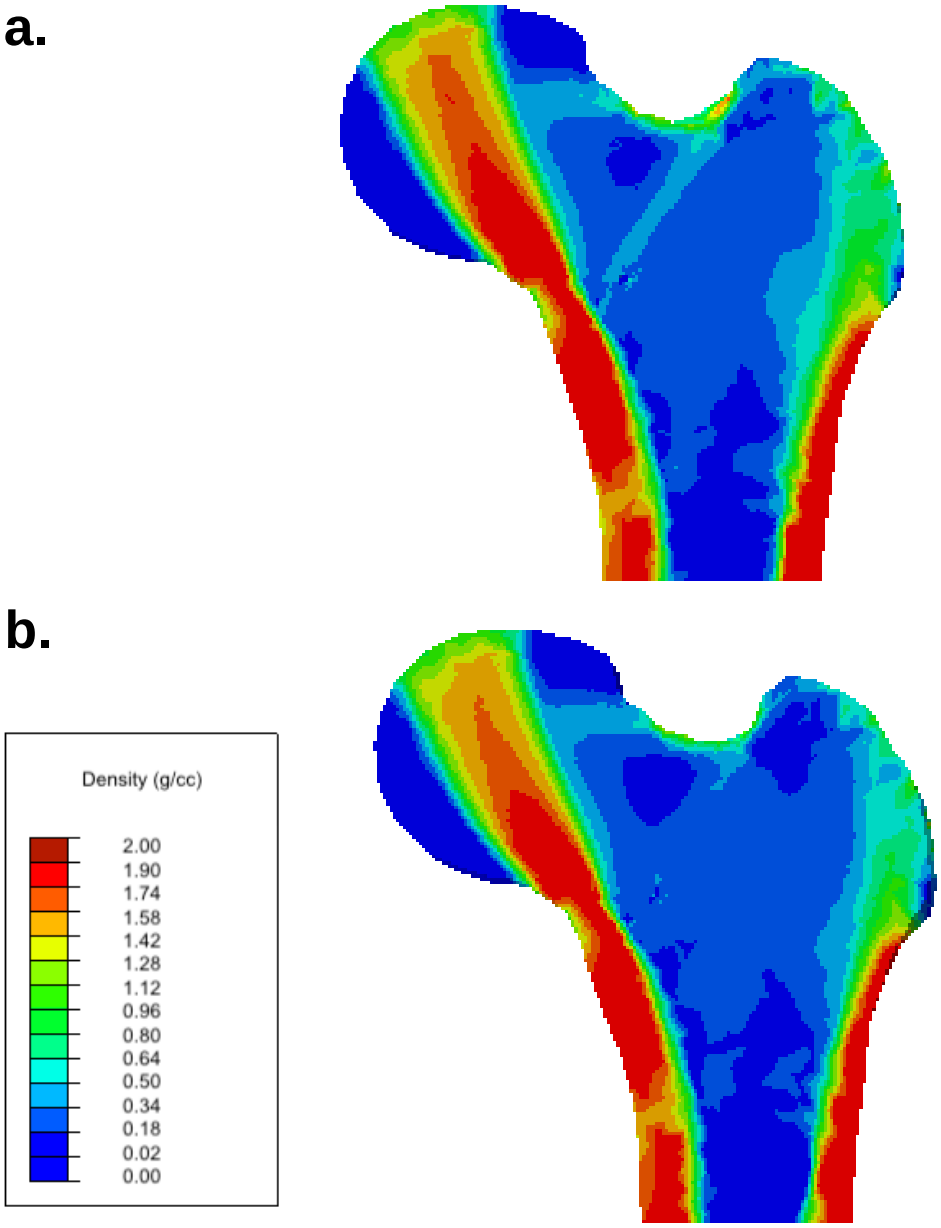

Figure 3.4 Superior neck density in (a) male marathon model and (b) female marathon model

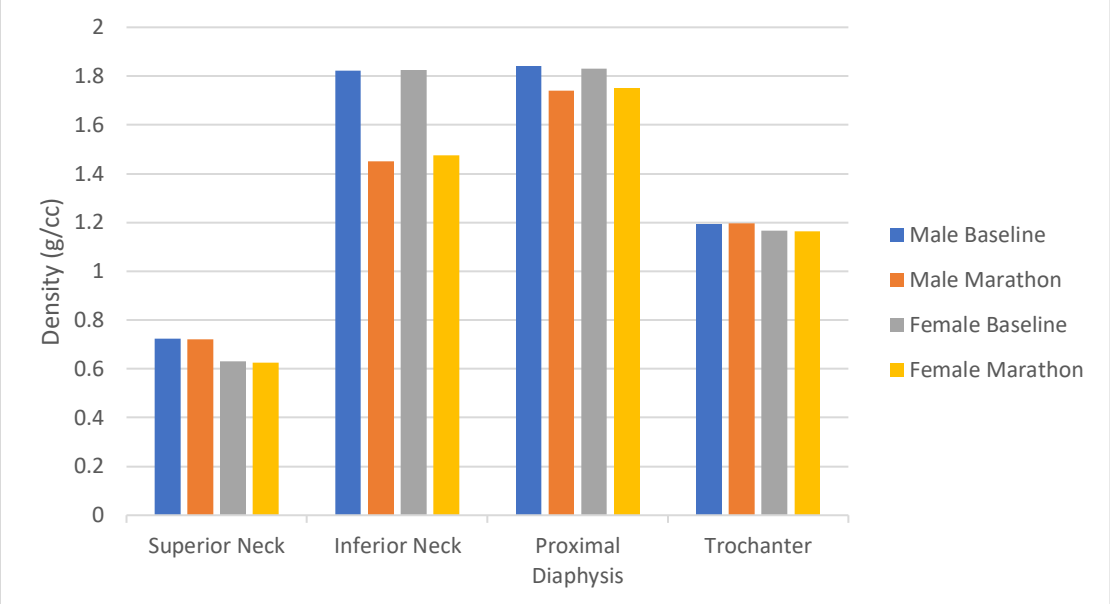

Figure 3.5 Predicted femoral bone mineral density before and after marathon training

After marathon training, the models predicted an increase in axial strain at all regions of interest except for the male trochanter. The inferior neck was predicted to experience the greatest strain at both baseline (Male: -468 με, Female: -457 με) and after marathon training (Male: -1270 με, Female: -1133 με). This region also experienced the greatest percent increase in strain after marathon training (Male: 92%, Female: 85%). Axial strain results for all models are shown below in Figure 3.6. Axial strain was measured in microstrain (Microstrain = Strain × 10^6). Tensile strain was defined as positive and compressive strain was defined as negative.

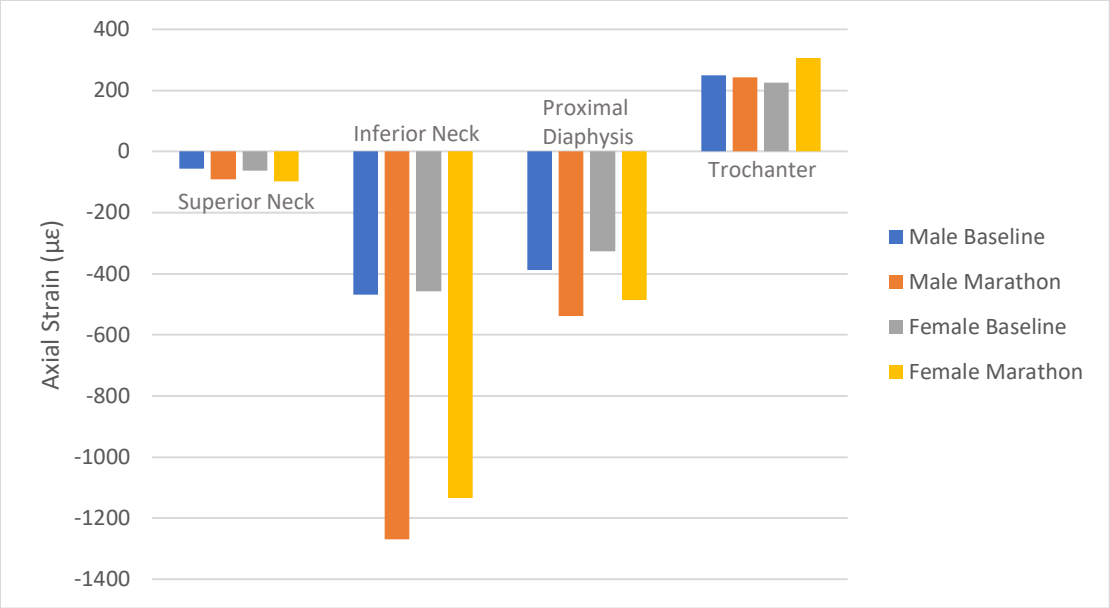

Figure 3.6 Predicted femoral axial strain before and after marathon training. (Microstrain = Strain × 10^6. Tensile strain is positive and compressive strain is negative.)

The inferior neck and proximal diaphysis were predicted to have the most damage before and after marathon training. Damage was predicted to increase in all regions after marathon training, with the greatest percent increase at the superior and inferior neck. Damage predicted after marathon training significantly increased above baseline by 97-136% at the superior neck and 91-97% at the inferior neck. Figure 3.7 shows the increase in inferior neck damage for the male model following marathon training. The increase in superior neck damage was especially greater for females (Male: 97%, Female: 136%), as shown in Figure 3.8. Damage results are shown in Figure 3.9 below.

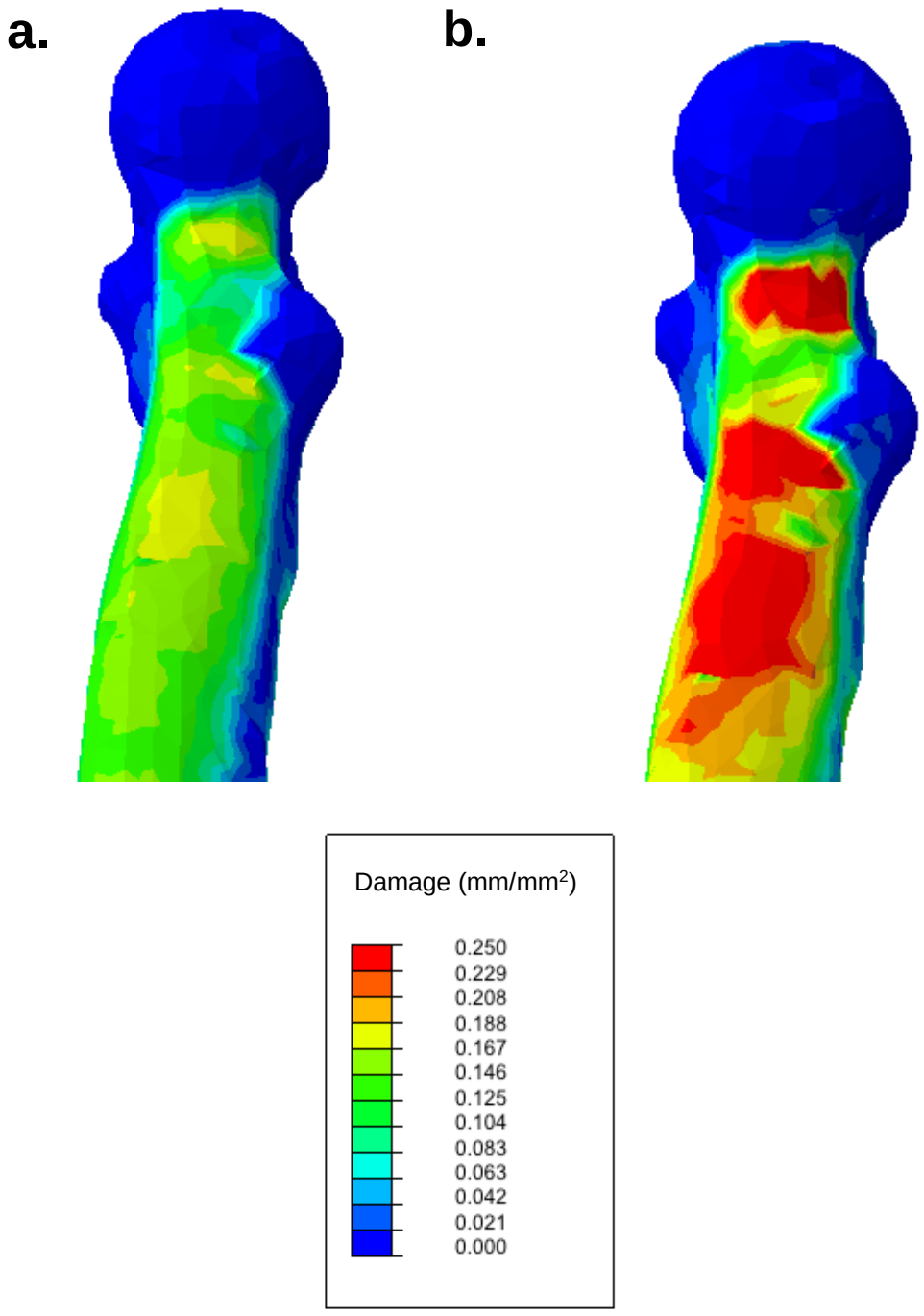

Figure 3.7 Predicted inferior neck damage for male model (a) at baseline and (b) after marathon training. (Damage is reported as total crack length (mm) per section area of bone (mm^2)).

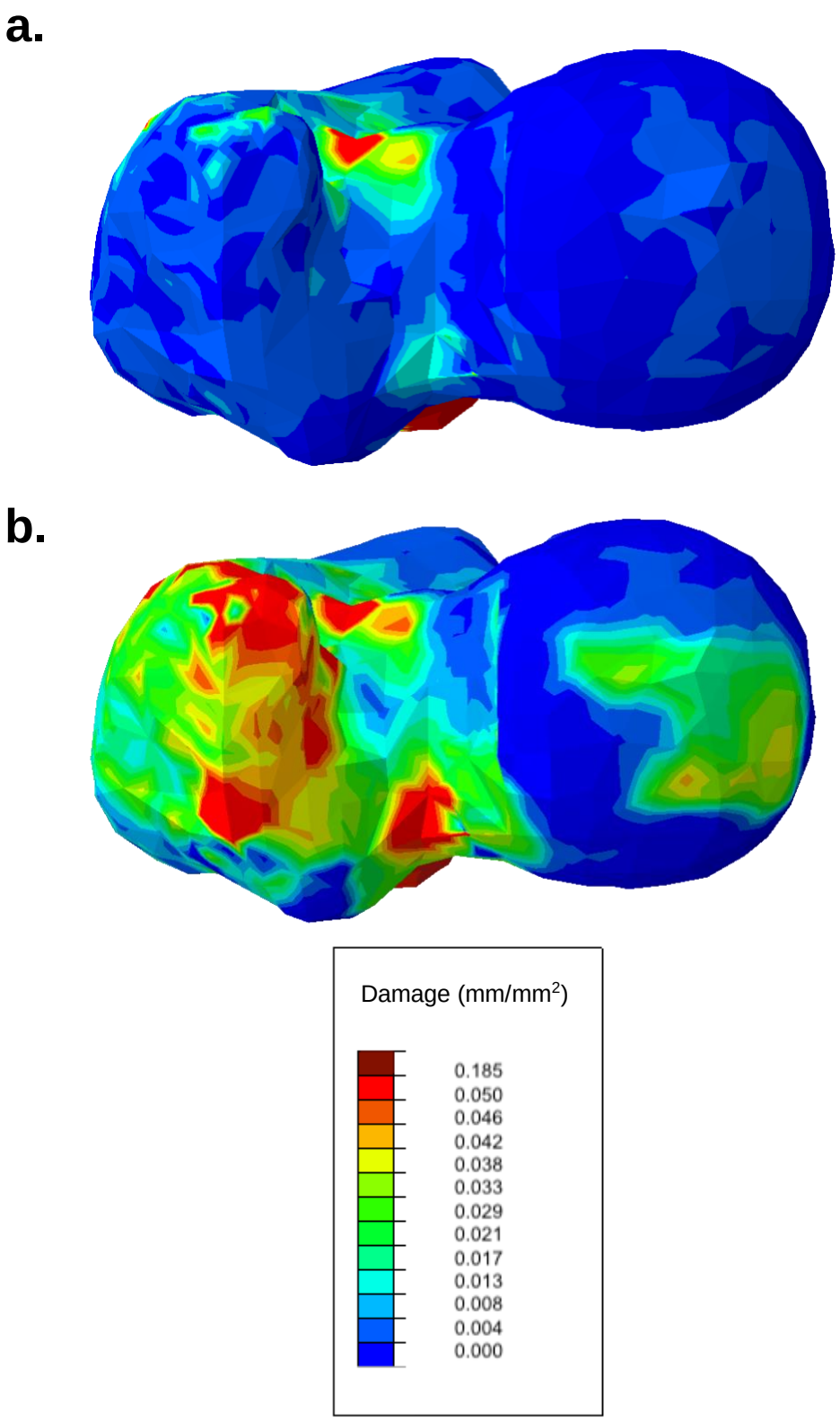

Figure 3.8 Predicted superior neck damage for female model (a) at baseline and (b) after marathon training. (Damage is reported as total crack length (mm) per section area of bone (mm^2)).

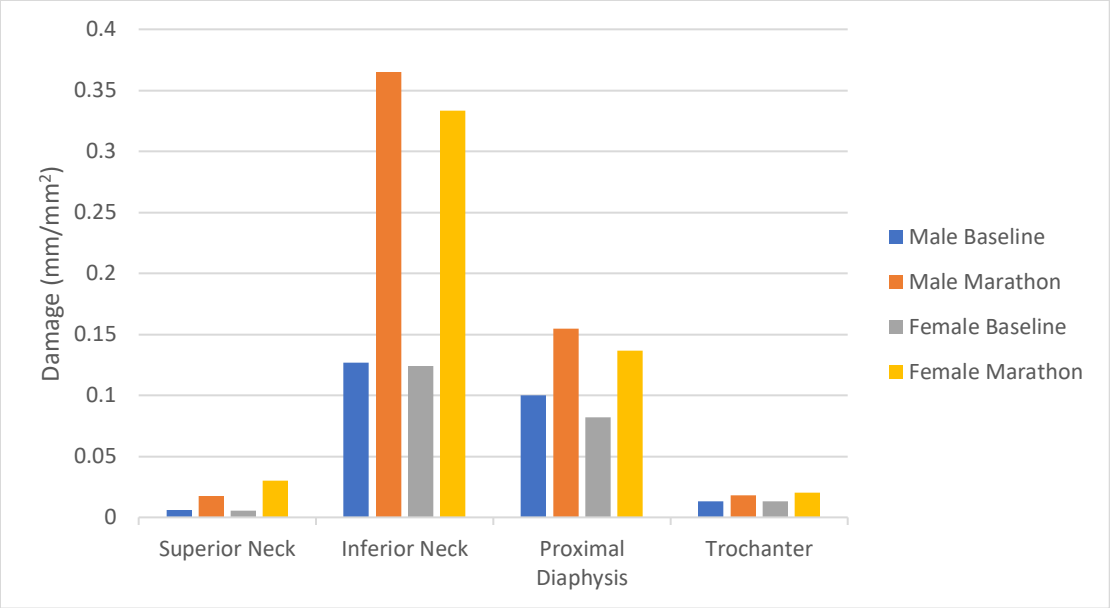

Figure 3.9 Predicted femoral damage before and after marathon training. (Damage is reported as total crack length (mm) per section area of bone (mm^2)).

Males and females were predicted to have similar percent changes in BMU remodeling activity before and after marathon training. The baseline model predicted the greatest activation frequency at the superior neck (Male: 0.0673 BMU/mm^2/day, Female: 0.0789 BMU/mm^2/day). In contrast, the marathon training model predicted the greatest activation frequency at the inferior neck (Male: 0.299 BMU/mm^2/day, Female: 0.283 BMU/mm^2/day). Marathon training was predicted to decrease BMU remodeling activity most significantly at the superior neck. Activation frequency decreased by approximately 200% at the superior neck and trochanter but increased at the inferior neck and proximal diaphysis after marathon training. Figure 3.10 shows the predicted increase in activation frequency at the inferior neck and proximal diaphysis. BMU remodeling activity for all models are shown below in Figure 3.11.

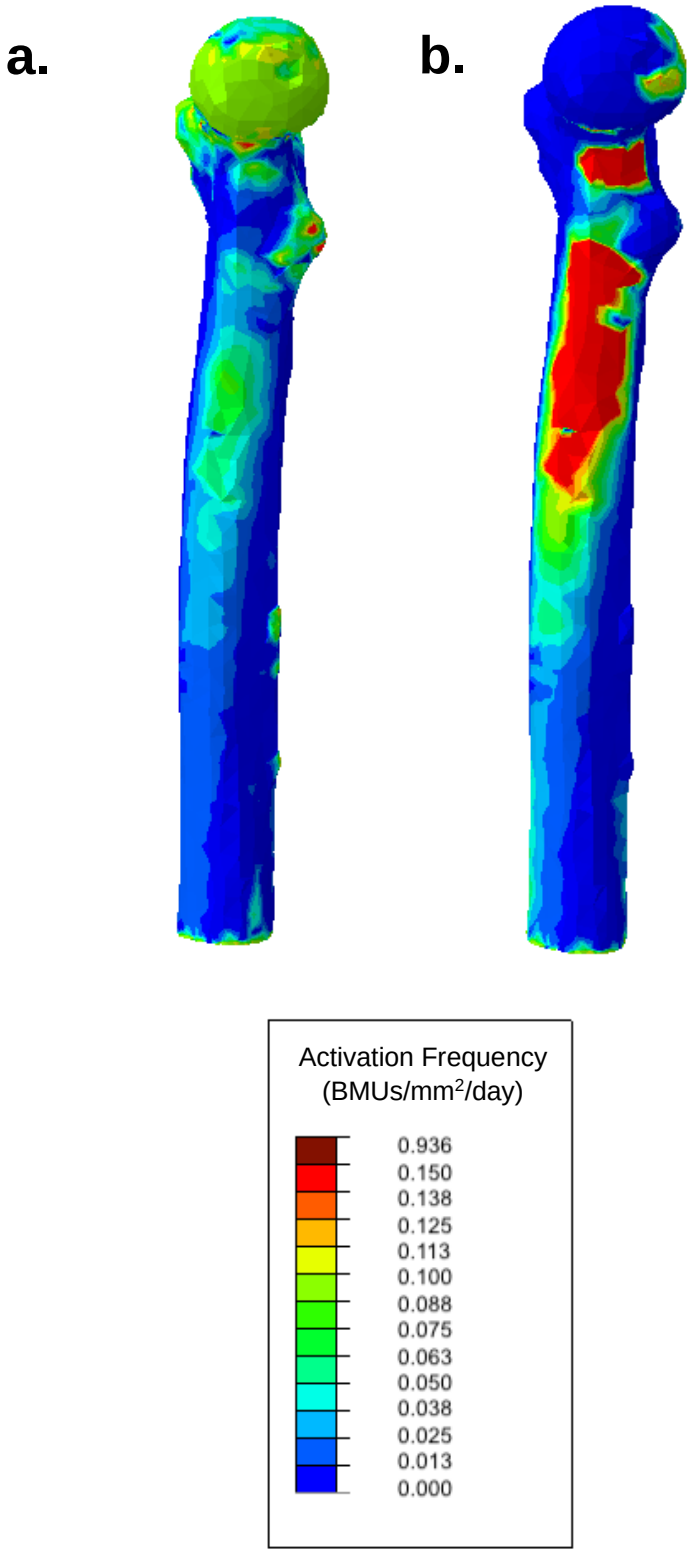

Figure 3.10 Predicted activation frequency for male model (a) at baseline and (b) after marathon training

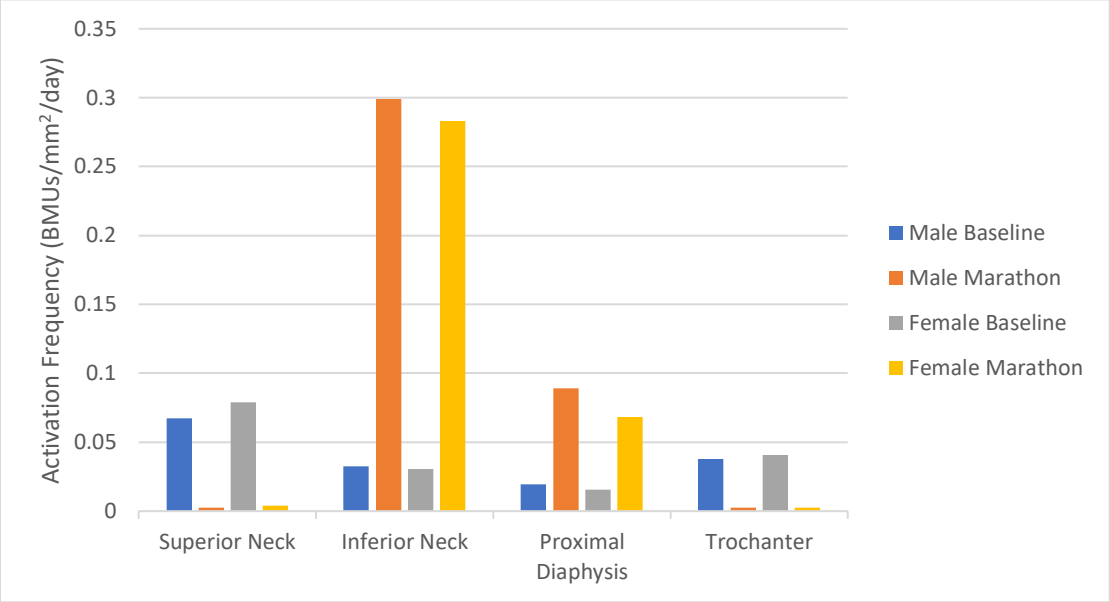

Figure 3.11 Predicted BMU remodeling activity before and after marathon training

Axial strain, bone mineral density, damage, and BMU remodeling activity at regions of interest in the baseline and marathon loading cases are summarized in Table 3.2 for males and Table 3.3 for females. Positive strain is defined as tensile and negative strain is defined as compressive. Individual contour plots for each model can be found in Appendix D.

Table 3.2 Male finite element model results before and after marathon training

Zone	Axial Strain* (microstrain, με)		Density (g/cm^3)		Damage (mm/mm^2)		Activation Frequency (BMUs/mm^2/day)	
	Baseline	Marathon	Baseline	Marathon	Baseline	Marathon	Baseline	Marathon
Superior neck	-57.12	-90.49	0.7239	0.7222	0.0061	0.0174	0.0673	0.0023
Inferior Neck	-467.9	-1270	1.821	1.451	0.1268	0.3649	0.0323	0.2990
Proximal Diaphysis	-388.5	-537.9	1.843	1.740	0.1000	0.1546	0.0196	0.0893
Trochanter	249.9	243.9	1.194	1.196	0.0134	0.0179	0.0377	0.0024

* Positive strain is tensile, negative strain is compressive

Table 3.3 Female finite element model results before and after marathon training

Zone	Axial Strain* (microstrain, με)		Density (g/cm^3)		Damage (mm/mm^2)		Activation Frequency (BMUs/mm^2/day)	
	Baseline	Marathon	Baseline	Marathon	Baseline	Marathon	Baseline	Marathon
Superior neck	-62.95	-98.08	0.6309	0.6265	0.0057	0.0299	0.0789	0.0038
Inferior Neck	-457.4	1133	1.826	1.475	0.1243	0.3336	0.0304	0.2831
Proximal Diaphysis	-327.7	-485.2	1.831	1.752	0.0822	0.1364	0.0156	0.0682
Trochanter	225.5	306.2	1.166	1.165	0.0133	0.0204	0.0406	0.0027

* Positive strain is tensile, negative strain is compressive

Chapter 4

DISCUSSION

4.1 Interpreting Finite Element Analysis Results

4.1.1 Differences between Baseline and Marathon Training Models

It was hypothesized that marathon training would decrease bone strength at the superior neck, inferior neck, proximal diaphysis, and trochanter (Figure 4.1). Table 4.1 summarizes the predicted changes in femur bone parameters following marathon training. The finite element model predicted greater damage at all regions of interest following marathon training. The model predicted higher strain and lower bone mineral density after marathon training at all regions of interest except for the male trochanter. Strain magnitude is inversely related to fatigue life of bone [13], so the increased strain seen in the finite element model may indicate weaker bone at greater risk of fracture. Increased damage from running activates the bone remodeling response, which contributes to a decrease in bone mineral density as damaged bone is resorbed. Femoral fractures are 2.6 times more common for every standard deviation reduction of femoral bone mineral density below the age-adjusted mean [10]. The increased damage, increased strain, and decreased bone mineral density predicted by the model support the hypothesis that marathon training decreases bone strength at these regions of interest.

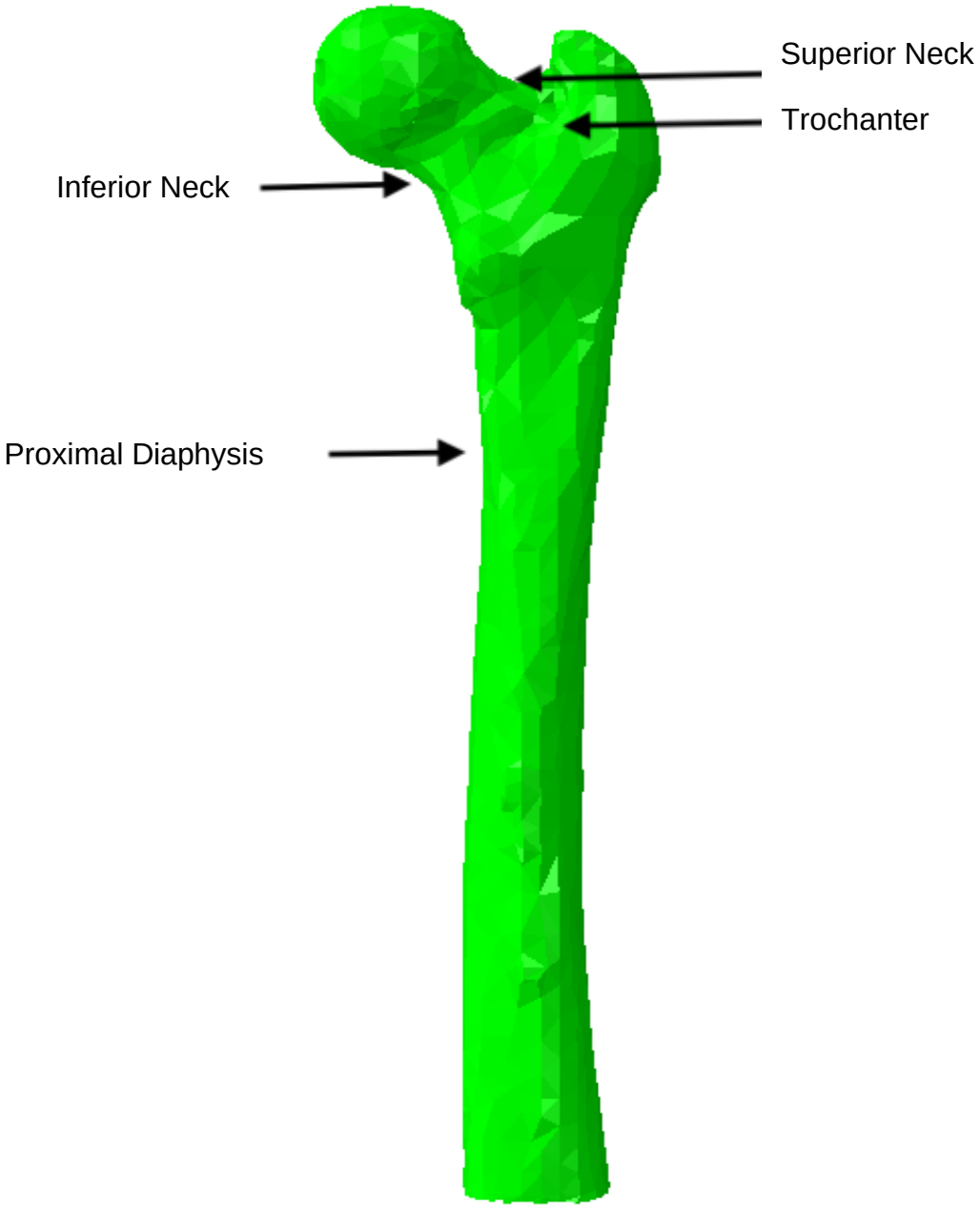

Figure 4.1 Regions of interest with predicted decrease in strength following marathon training

Table 4.1 Summary of predicted changes in femur parameters of interest following marathon training

	Superior Neck	Inferior Neck	Proximal Diaphysis	Trochanter
Axial Strain	Male: ↑	Male: ↑	Male: ↑	Male: ↓
	Female: ↑	Female: ↑	Female: ↑	Female: ↑
Density	Male: ↓	Male: ↓	Male: ↓	Male: ↑
	Female: ↓	Female: ↓	Female: ↓	Female: ↓
Damage	Male: ↑	Male: ↑	Male: ↑	Male: ↑
	Female: ↑	Female: ↑	Female: ↑	Female: ↑
Activation Frequency	Male: ↓	Male: ↑	Male: ↑	Male: ↓
	Female: ↓	Female: ↑	Female: ↑	Female: ↓

The inferior neck may be at greater risk of fracture due to higher strain, higher damage, and lower bone mineral density predicted after marathon training. The inferior neck had the highest amount of strain in all models and the greatest percent increase in strain after marathon training (Male: 92%, Female: 85%). This region was also predicted to have the most damage, as well as the largest drop in bone mineral density after marathon training (Male: 23%, Female: 21%). Decreased bone mineral density may increase risk of inferior neck fracture. A study by Pouilles et al. found that average bone mineral density of military recruits with femoral neck fractures was 10% lower than in those without fractures [49]. Weaker inferior neck bone properties predicted by the model align

with clinical observations that femoral neck fractures make up 40% to 50% of all hip fractures [50]. A study by Edwards et al. determined that the locations of maximum femoral loads matched the most common clinically observed stress fracture locations [46]. The femoral neck transmits thigh and pelvis muscle loads to the hip joint. High compressive loads at the inferior neck combined with weak bone properties may contribute to fracture.

In addition to inferior neck weakness, the finite element model predicted changes in location of peak BMU activation frequency following marathon training. The superior neck was predicted to have the highest activation frequency at baseline. After marathon training, activation frequency was predicted highest at the inferior neck, followed by the proximal diaphysis. The inferior neck and proximal diaphysis also contained the most damage and axial strain in both baseline and marathon training models. The predicted increase in BMU activation frequency may have been stimulated by high damage and strain, which increased in these regions after marathon training. Remodeling temporarily reduces bone's load-bearing ability following resorption of old bone before the cavity is refilled with new bone. The newly deposited bone is also initially weaker because it has not yet been mineralized. Therefore, increased remodeling activity combined with high loads may put the inferior neck and proximal diaphysis at risk of fracture during marathon training.

4.1.2 Differences between Male and Female Models

It was hypothesized that females would have lower bone mineral density, higher remodeling activity, and more microdamage at the superior neck, inferior

neck, proximal diaphysis, and trochanter. The models predicted differences between male and female femur bone properties at the superior neck, trochanter, and proximal diaphysis. These differences suggest that females may be more prone to stress fracture at these regions following marathon training.

Females are predicted to have a weaker superior neck than males, and this weakness may become more severe following marathon training. Despite a lower body weight, the female was predicted to experience greater superior neck strain than males at baseline (Male: -57 με, Female: -62 με) and after marathon training (Male: -90 με, Female: -98 με). These strains are relatively small given that the estimated bone yield strain is 25,000 με [50], and the remodeling process can effectively repair microdamage when strains are between 1,500 to 10,000 με [51]. Therefore, it is not conclusive that this predicted increase in strain magnitude will increase likelihood of stress fracture, but the large number of repetition cycles of submaximal strains during marathon training may decrease bone strength. Females were also predicted to have 53% more damage (Female = 0.030 mm/mm^2, Male = 0.017 mm/mm^2) and 47% higher BMU activation frequency (Female = 0.0038 BMUs/mm^2/day, Male = 0.0023 BMUs/mm^2/day) than males at the superior neck following marathon training. Superior neck damage increased more notably in the female model after marathon training (Male: 97%, Female: 136%).

The predicted amounts of damage after marathon training were still relatively small, so they may not be significant enough to increase stress fracture risk. There is no definitive quantity of microdamage associated with stress

fracture development. The relationship between microdamage and bone strength is negatively exponential; a small increase in microdamage may significantly impact bone strength if the bone already has reached a level of reduced bone mineral density [52]. The following relationship between bone strength (MPa) and Cr.Dn (microcrack density, # of cracks/mm^2 of bone) was determined based on experimental studies of human vertebral bone:

$$Bone\ Strength = 4.84e^{-0.16*Cr.Dn}$$ (Equation 4)

Therefore, quantity of microcracks may predict bone strength, but this simple relationship does not account for the effects of bone remodeling or bone density. Stress fracture risk depends on interactions between microdamage, the remodeling response, and resulting bone strength. Microdamage activates the bone remodeling response, which decreases bone mineral density as damaged bone is resorbed. Bone stiffness and strength decrease exponentially with a decrease in bone mineral density. When there is less bone tissue to sustain loading, the remaining bone tissue is placed under increased strain, which activates a positive feedback loop of more microdamage, more remodeling, more bone loss, and more strain. Over time, this positive feedback loop may reach a threshold at which stress fracture is likely to occur [52]. In this way, a small increase in microdamage may be detrimental to bone strength over time. Based on the results of this model, it is inconclusive that the greater strain, damage, and bone remodeling activity predicted for females is significant enough to increase risk of superior neck fracture in females compared to males. These predicted

trends in bone material properties can only suggest that the bone becomes weaker, which could potentially increase likelihood of stress fracture over time.

These finite element model results support clinical observations that femoral neck fractures occur three times more in women [53]. While the inferior neck was a predicted location of weakness in both sexes, a weaker superior neck specific to females may contribute to higher incidence of fracture. Superior neck stress fractures are less favorable because they have a greater chance of propagation and delayed recovery, or non-union, compared to other regions [45]. While fatigue loading is the primary cause of stress fractures, weak hip abductor muscles are hypothesized to contribute to superior neck fractures [54]. Muscles disperse and share impact loads on bones [4]. Muscle fatigue or weakness takes away this protective action by transferring loads to bone, which increases fracture risk [26]. The gluteus medius and minimus are responsible for counterbalancing tensile forces at the superior neck, but tension on the femur increases as these muscles become fatigued. The gluteus medius muscle force were scaled up for females in the finite element model to represent greater activation, but the increase may not have been large enough to counterbalance tensile loads from running. This finite element model does not account for the effects of fatigue, but females who activate these muscles more during running may experience earlier gluteal muscle fatigue. Therefore, females may benefit from training programs that strengthen the abductor muscles to reduce superior neck tension and delay the onset of fatigue.

The trochanter was another suspected region of weakness in females. After marathon training, females were predicted to have greater axial strain at the trochanter than males (Male: -244 με, Female: -306 με). Strain at the trochanter was not significantly affected by marathon training in the male model, but the female model experienced a 30% increase from baseline. Weaker baseline bone properties could be a possible reason for this higher trochanter strain in the female model after marathon training. Since the female model had baseline muscle and joint pressure loads scaled to a lower body weight, the femur may have been unable to bear the higher volume and magnitude of marathon training loads. Closer analysis of bone mineral density at the trochanter shows that females have lower density than males before and after marathon training. A potential solution may be for females to gradually increase activity levels prior to beginning marathon training to develop stronger baseline bone properties.

Compared to the male model, the female trochanter was predicted to have greater damage and activation frequency after marathon training. Trochanter damage was predicted to increase by 43% from baseline in females and 30% from baseline in males. The gluteus medius insertion point is located at the trochanter, so the increased muscle force activation in this model may have contributed a larger increase in damage at this region following marathon training.

Although the female proximal diaphysis had less damage than the male in both baseline and marathon training models, females were predicted to have a greater increase in damage at this region following marathon training. The female

model exhibited a 50% increase in damage at the proximal diaphysis after marathon training, whereas the male exhibited a 43% increase. Prior studies have hypothesized that femoral stress fractures occurring at the proximal diaphysis, especially at the medial region, are more likely to occur when the hip abductor muscles responsible for resisting bending moment become fatigued [13]. Like the superior neck, this is another location in which insufficient abductor muscle forces may increase fracture risk by increasing loading on the bone.

4.2 Limitations

The femur CT scan used in this study was taken from a male subject, which does not consider sex differences in bone size or structure. Typical bone size is greater in males, and females have smaller femur bone section moduli that are weaker under bending loads [55], [56]. On the other hand, the greater bone size in males is accompanied by a higher body weight and loads on the femur, which was accounted for in the finite element model. The geometrical features of a smaller femoral head radius and wider pelvis typically seen in females have the greatest impact on hip joint loading [15], [17]. These differences were adjusted for in the female finite element model by increasing the joint pressure and abductor muscle angle. Other structural differences observed in females include a shorter femoral neck and thinner femoral shaft [57]. A study by Vahdati et al. found that subject-specific differences in loading conditions of the hip joint and muscle forces had a larger effect on accurately predicting bone density than individualized geometry [58]. Therefore, inaccuracies from using a male femur CT scan are not expected to significantly impact the results of this

study, but sex-specific bone geometry should be used to improve accuracy. Validation of the model could also have been improved by collecting strain data from cadaver femurs belonging to male and female marathon runners, or subjects of a similar body weight as in the model.

While this model can predict damage and increases in damage following marathon training, there is no quantity of damage necessarily associated with an increase in fracture risk. Stress fractures are caused by the interaction between mechanical loads and risk factors [13]. Extrinsic risk factors such as running surface, footwear, and training intensity can be modified by the athlete to prevent fracture. Intrinsic factors such as musculature, fitness level, body fat, and hormonal variations are more difficult to control [8]. Females suffering from the Female Athlete Triad (disordered eating, amenorrhea, and osteoporosis) have an especially high risk of bone fracture [24]. This disorder is often unrecognized but can have severe consequences on bone strength in female runners. Calcitonin, parathyroid hormone, vitamin D, and estrogen regulate the bone remodeling process [59], but the effects of these factors were not included in the bone remodeling algorithm. For example, estrogen inhibits bone resorption by decreasing the number of active BMUs, and decreased estrogen levels in women after menopause increases their likelihood of developing stress fractures. Older female runners may have a higher fracture risk than younger female runners due to this hormonal change, but the finite element model developed in this thesis is unable to capture this difference. This finite element model only studies the

effects of mechanical loads; the complex interaction of other risk factors and their influence on stress fracture probability are not accounted for.

Although the remodeling algorithm accounted for biological and mechanical processes of bone remodeling, these parameters were selected based on values for an average individual. Individuals may have different remodeling periods, remodeling rates, resorption areas, and formation areas depending on their age and sex. Prior studies suggest that marathon runners may have different remodeling parameters than individuals who do not perform distance running. Frost determined that marathon runners have less bone mass than weight lifters even though they have a high amount of microdamage conducive to remodeling because marathon runners have smaller muscles that place less strain on the bone [50]. A study by O'Kane measured levels of NTx peptide, a molecular marker associated with bone resorption, in college endurance athletes and a control population that did not perform endurance sports [60]. This study found that both male and female distance runners had significantly higher levels of molecular markers associated with bone resorption than the control group. Therefore, the average bone remodeling parameters used in this study may not be representative of the marathon runner population.

4.3 Future Steps

Mechanisms of load reduction, such as gait training, are potential ways to prevent femoral stress fracture [54], [61], [62]. Crowell and Davis found that gait retraining immediately reduced vertical force loading rates and peak impact at the tibia, effectively reducing fracture risk [62]. A similar method of gait retraining

may be applied to the femur. Since hip and pelvis kinematics directly influence hip contact force, specific gait patterns may be introduced to reduce this load [61]. Gait patterns that reduce the hip abduction angle, which is naturally higher in females due to a wider pelvis, may decrease the hip contact force. Reducing stride length may also reduce likelihood of stress fracture. A study by Edwards found that a 10% reduction in stride length significantly reduced fracture risk at the tibia [13]. Reducing stride length increases the number of loading cycles required for a given mileage, but the benefits of reducing strain outweigh the detriment of more loading cycles [13]. In a future study, motion analysis could be performed on a female subject undergoing gait retraining. Joint and muscle loads after gait retraining could be incorporated into this finite element model to study the effectiveness of this injury prevention method on reducing bone damage.

Stress fractures frequently occur with overtraining or changes in a training routine [4]. A study found that increasing running mileage beyond 20 miles per week was associated with an increased risk of stress fracture [45]. Stress fractures in runners also tend to occur during the first two through eight weeks of a new training regimen [13]. Future work could be done to analyze bone properties at various time periods during the marathon training schedule, such as biweekly until race day. These results could help reveal if there is a particular week of training associated with large changes in strain, damage, density, or activation frequency. The nature of marathon racing requires a high volume of training, but certain training schedules may be more beneficial for preventing stress fractures than others. Hazelwood et al. found that varying daily running

mileage and incorporating rest periods minimized stress fracture risk compared to daily running for the same total mileage [27]. A future study could analyze the effectiveness of varying mileage per day and frequency of rest periods on reducing bone damage. The results from this study could help determine if one type of training plan is more beneficial to females or males in preventing stress fracture.

This model also assumed that all running was done at the same pace. A more realistic marathon training model would include the effects of different running speeds, such as during endurance versus sprinting workouts. Vastus lateralis and gluteal muscle activation increase with running speed, and this increase is more significant in females [18]. These speed-dependent muscle activation patterns may affect the remodeling process by altering loads on the bone. A future study could incorporate different running speeds to determine if this affects the likelihood of femoral stress fracture in males and females.

Chapter 5

CONCLUSIONS

The purpose of this thesis was to develop a three-dimensional femur finite element model simulating marathon training to predict regions at risk of stress fracture. This model was then used to determine if the higher risk of femoral stress fractures observed in female runners could be attributed to bone remodeling influenced by sex-specific loading conditions. In terms of predicting stress fracture risk, the model outputs strain and bone material properties (density, damage, activation frequency) that reflect bone strength. In terms of comparing male to female runners, the model includes loading differences caused by varying muscle activation patterns and hip geometry. The finite element model is validated to experimental cadaveric femur data. Marathon training was predicted to increase bone damage at all regions of interest (superior neck, inferior neck, proximal diaphysis, trochanter). Increased axial strain and decreased density were predicted at all regions except for the trochanter in the male model, with the inferior neck most greatly affected. Bone remodeling activation was predicted to increase at the inferior neck and trochanter but decrease at the superior neck and proximal diaphysis. When analyzing differences between sexes, females were predicted to have a greater increase in damage at the superior neck, trochanter and proximal diaphysis compared to males.

While the observations from the finite element model are unable to quantify fracture risk, they provide insight into which femoral regions are prone to

damage and bone weakness associated with stress fracture development. The inferior neck is anticipated to be a weak region for both males and females, and this weakness is predicted to increase with marathon training. Marathon training may have a significant effect on the location of peak bone remodeling activity, which is predicted at the inferior neck and proximal diaphysis. Females are predicted to have greater bone weakness than males at the superior neck, trochanter, and proximal diaphysis. Potential causes for these sex-based differences in bone strength include the greater abductor muscle activation in females and weaker baseline bone properties due to a lower female bodyweight.

In a future study, sex-specific femur bone geometry should be used for the finite element models. It was assumed that adapting sex-specific loads would account for some differences in bone geometry, but using male and female femur CT scans would improve accuracy of the results. This model only predicts the effects of the mechanical loading environment on bone remodeling and fails to recognize other risk factors, such as footwear, hormone levels, and type of training regimen. Despite these limitations, this finite element model successfully predicts changes in femoral axial strain, bone mineral density, damage, and activation frequency for males and females after marathon training.

BIBLIOGRAPHY

[1] Andersen, J.J. (2020). Marathon Statistics 2019 Worldwide. Retrieved September 13, 2020 from https://runrepeat.com/research-marathon-performance-across-nations

[2] Vaughan, C.L. (1984). Biomechanics of running gait. *Crit Rev Biomed Eng., 12(1),* 1-48. Retrieved September 13, 2020 from https://pubmed.ncbi.nlm.nih.gov/6394212/

[3] Robertson, G.A., Wood, A.M. (2017). Lower limb stress fractures in sport: Optimizing their management and outcome. *World J Orthop, 8(3),* 242-255. https://doi.org/10.5312/wjo.v8.i3.242

[4] Astur, D.C., Zanatta, F., Arliani, G.G., Moraes, E.R., Pochini, A.d. Ejnisman, B. (2015). Stress Fractures: definition, diagnosis, and treatment. *Rev Bras Orto, 51(1),* 3-10. https://doi.org/10.1016/j.rboe.2015.12.008

[5] Mohsin, S., O'Brien, F.J., Lee, T.C. (2006). Microcracks in compact bone: a three-dimensional view. *Journal of Anatomy, 209(1),* 119-124. https://doi.org/10.1111/j.1469-7580.2006.00554.x

[6] Hazelwood, S.J., Martin, R.B., Rashid, M.M., et al. (2001). A mechanistic model for internal bone remodeling exhibits different dynamic responses in disuse and overload. *Journal of Biomechanics, 34,* 299-308.

[7] King, D. (2004). Bone Remodeling. Carbondale, IL: Southern Illinois School of Medicine Retrieved from http://www.siumed.edu/~dking2/ssb/remodel.htm

[8] Hughes, J.M., Popp, K.L., Yanovich, R., Bouxsein, M.L., Mathney, R.W. (2016). The role of adaptive bone formation in the etiology of stress fracture. *Exp Biol Med (Maywood), 242(9),* 897-906. https://doi.org/10.1177/1535370216661646

[9] Robertson, G.A., Wood, A.M. (2017). Femoral Neck Stress Fractures in Sport: A Current Concepts Review. *Sports Med Int Open, 1(2),* E58-E68. https://doi.org/10.1055/s-0043-103946

[10] Biz, C. Berizzi, A., Crimí, A. et al. (2017). Management and treatment of femoral neck stress fractures in recreational runners: a report of four cases and review of the literature. *Acta Biomed, 88(4),* 96-106. http://doi.org/10.23750/abm.v88i4-S.6800

[11] Wentz, L., Liu, P., Haymes, E., Ilich, J.Z. (2011). Females Have a Greater Incidence of Stress Fractures Than Males in Both Military and Athletic Populations: A Systematic Review. *Military Medicine, 176,* 420-430. https://doi.org/10.7205/miomed-d-10-00322

[12] Callahan, L.R. (2000). Stress Fractures in Women. *Clinics in Sports Medicine, 19(2),* 303-314. https://doi.org/10.1016/S0278-5919(05)70205-2

[13] Edwards, W.B. (2009). *Internal structural loading of the lower extremity during running: Implications for skeletal injury.* [Unpublished Doctoral dissertation]. Iowa State University.

[14] Ferber, R., Davis, I.M., Williams III, D.S. (2003). Gender differences in lower extremity mechanics during running. *Clinical Biomechanics, 18,* 350-357. https://doi.org/10.1016/S0268-0033(03)00025-1

[15] Iglic, A., Daniel, M., Kralj-Iglic, V., Antolic, V., Jaklic, A. (2001). Peak hip-joint contact stress in male and female populations. Journal of Musculoskeletal Research, 5(1). 17-21. http://doi.org/10.1142/S0218957701000350

[16] Kersnič, B., Iglič, A., Kralj-Iglič, V., Srakar, F., Antolič, V. (1996). Increased incidence of arthrosis in women could be related to femoral and pelvic shape. *Arch Orthrop Trauma Surg, 116,* 345-347. Retrieved August 16, 2020 from https://link.springer.com/content/pdf/10.1007/BF00433987.pdf

[17] Kralj-Iglič, V. (2015). Validation of Mechanical Hypothesis of hip Arthritis Development by HIPSTRESS Method. *Osteoarthritis – Progress in Basic Research and Treatment* (Chapter 7). https://doi.org/10.5772/59976

[18] Chumanov, E.S., Wall-Scheffler, C., Heiderscheit, B.C. (2008). Gender differences in walking and running on level and inclined surfaces. *Clinical Biomechanics, 23,* 1260-1268. https://doi.org/10.1016/j.clinbiomech.2008.07.011

[19] Sinclair, J., Greenhalgh, A., Edmundson, C.J., Brooks, D., Hobbs, S.J. (2012). Gender Differences in the Kinetics and Kinematics of Distance Running: Implications for Footwear Design. *International Journal of Sports Science and Engineering, 6(2),* 118-128. Retrieved August 16, 2020 from https://www.researchgate.net/publication/229442418_Gender_Differences_in_the_Kinetics_and_Kinematics_of_Distance_Running_Implications_for_Footwear_Design

[20] Ferber, R., Davis, I.M., Williams, D.S. (2003). Gender differences in lower extremity mechanics during running. *Clinical Biomechanics, 18,* 350-357. http://doi.org/10.1016/S0268-0033(03)00025-1

[21] Willson, J.D., Petrowitz, I., Butler, R.J., Kernozek, T.W. (2012). Male and female gluteal muscle activity and lower extremity kinematics during running. *Clin Biomech, 27(10),* 1052-1057. https://doi.org/10.1016/j.clinbiomech.2012.08.008

[22] (2016). OpenStax, Biology. Female and Male Pelvis. Rice University. Retrieved from https://cnx.org/contents/GFy_h8cu@10.53:sw1Ot2vk@3/Types-of-Skeletal-Systems

[23] Arab, A.M., Nourbakhsh, M.R. (2010). The relationship between hip abductor muscle strength and iliotibial band tightness in individuals with low back pain. *Chiropractic & Osteopathy, 18(1).* https://doi.org/10.1186/1746-1340-18-1

[24] Casey, E., Rho, M., Press, J. (2016). Sex Differences in Sports Medicine. Springer Publishing Company, LLC.

[25] Neely, F.G. (1998). Intrinsic Risk Factors for Exercise-Related Lower Limb Injuries. *Sports Med, 26,* 253-263. https://doi.org/10.2165/00007256-199826040-00004

[26] Burr, D.B. (1997). Bone, Exercise, and Stress Fractures. *Exercise and Sport Science Reviews, 25(1),* 171-194. Retrieved September 3, 2020 from https://journals.lww.com/acsmessr/Citation/1997/00250/7_Bone,_Exercise,_and_Stress_Fractures.9.aspx

[27] Hazelwood, S.J., Castillo, A.B. (2006). Simulated effects of marathon training on bone density, remodeling, and microdamage accumulation of the femur. *International Journal of Fatigue, 29,* 1057-1064. https://doi.org/10.1016/j.ijfatigure.2006.10.001

[28] Deuel, C.R. (2007). *Development of an Adaptive 3-D Model of the Human Femur to Simulate Bone Remodeling Following Hip Resurfacing and Total Hip Arthroplasties.* [Unpublished Doctoral dissertation]. University of California Davis.

[29] Viceconti, M., Bellingeri, L., Cristofolini, L., Toni, A. (1998). A comparative study on different methods of automatic mesh generation of human femurs. *Med Eng Phys, 20(1),* 1-10. https://doi.org/10.1016/s1350-4533(97)00049-0

[30] Whalen, R.T., Carter, D.R. (1988). Influence of Physical Activity on the Regulation of Bone Density. *J. Biomechanics, 21(10),* 825-837. https://doi.org/10.1016/0021-9290(88)90015-2

[31] Zioupos, P., Cook, R.B., Hutchinson, J.R. (2008). Some basic relationships between density values in cancellous and cortical bone. *J. Biomech, 41(9),* 1961-1968. https://doi.org/10.1016/j.jbiomech.2008.03.025

[32] McLeish, R.D., Charnley, M.J. (1970). Abduction forces in the one-legged stance. *Journal of Biomechanics, 3(2),* 195-209. https://doi.org/10.1016/0021-9290(70)90006-0

[33] Christensen, C.L., Ruhling, R.O. (1983). Physical Characteristics of Novice and Experienced Women Marathon Runners. *Brit. J. Sports Med., 17(3),* 166-171. Retrieved August 20, 2020 from https://www.ncbi.nlm.nih.gov/pmc/articles/PMC1859165/pdf/brjsmed00247-0020.pdf

[34] Tanda, G., Knechtle, B. (2013). Marathon performance in relation to body fat percentage and training indices in recreational male runners. *Open Access J Sports Med, 4*, 141-149. https://doi.org/10.2147/OAJSM.S44945

[35] Martin, R.B., Burr, D.B., Sharkey, N.A., Fyhrie, D.P. (2015). *Skeletal Tissue Mechanics* (Chapter 1). New York: Springer-Verlag

[36] Woyski, D., Olinger, A., Wright, B. (2013). Smaller insertion area and inefficient mechanics of the gluteus medius in females. *Surgical and Radiologic Antomy, 35, 713-719.* https://doi.org/10.1007/s00276-013-1096-2

[37] (2020). Diagram of a normal hip. Retrieved from http://cityhospitaldehradun.com/arthrits/hip-arthritis/diagram-normal-hip/

[38] Deuel, C.R., Jamali, A.A., Stover, S.M., Hazelwood, S.J. (2009). Alterations in femoral strain following hip resurfacing and total hip replacement. *The Journal of Bone & Joint Surgery, 91(1),* 124-130. https://doi.org/10.1302/0301-620X.91B1.20789

[39] Giarmatzis, G., Jonkers, I., Wesseling, M., Van Rossom, S., Verschueren, S. (2015). Loading of Hip Measured by Hip Contact Forces at Different Speeds of Walking and Running. *Journal of Bone and Mineral Research, 30(8), 1431-1440.* https://doi.org/10.1002/jbmr.2483

[40] van den Bogert, A.J., Read, L., Nigg, B.M. (1998). An analysis of hip joint loading during walking, running, and skiing. *Medicine and Science in Sports and Exercise, 31(1),* 131-142. https://doi.org/10.1097/00005768-199901000-00021

[41] Thelen, D.G., Heiderscheit, B.C. (2014). Hip Muscle Loads During Running at Various Step Rates. *Journal of Orthopaedic and Sports Physical Therapy, 44(10),* 1-30. https://doi.org/10.2519/jospt.2014.5575

[42] Hobson, B. (2018). A brand new, 16 week marathon training plan for intermediate runners. *Runner's World.* Retrieved August 16, 2020 from https://www.runnersworld.com/uk/training/marathon/a776015/try-this-brand-new-16-week-marathon-training-plan/

[43] Tudor-Locke, C., Craig, C.L., Brown, W.J. et al. (2011). How many steps/day are enough? for adults. *Int J Behav Nutr Phys Act* 8, 79. https://doi.org/10.1186/1479-5868-8-79

[44] *Stanford Healthcare, Types of Hip Fractures.* https://stanfordhealthcare.org/medical-conditions/bones-joints-and-muscles/hip-fracture/types.html

[45] Kiel, J., Kaiser, K. (2020). Stress Reaction and Fractures. *StatPearls Publishing* [Internet]. Treasure-Island, Florida. Retrieved August 24, 2020 from https://www.ncbi.nlm.nih.gov/books/NBK507835/

[46] Edwards W.B., Gillette, J.C., Thomas, J.M., et al. (2008). Internal femoral forces and moments during running: Implications for stress fracture development. Clinical Biomechanics, 23(10). 1269-1278. https://doi.org/10.1016/j.clinbiomech.2008.06.011

[47] Bergmann, G., Deuretzbacher, G., Heller, M., Graichen, F., Rohlmann, A., Strauss, J., Duda, G.N. (2001). *Journal of Biomechanics, 34(7),* 859-871. https://doi.org/10.1016/S0021-9290(01)00040-9

[48] Turner CH, Anne V, Pidaparti RM. A uniform strain criterion for trabecular bone adaptation: do continuum-level strain gradients drive adaptation? J

Biomech 1997;30- 6:555-63. https://doi.org/10.1016/s0021-9290(97)84505-8

[49] Pouilles, J.M., Bernard, J., Tremoillères, Louvet J.P., Ribot, C. (1989). Femoral bone density in young male adults with stress fractures. *Bone, 10(2),* 105-108. https://doi.org/10.1016/8756-3282(89)90006-9

[50] Frost, H.M. Why do Marathon Runners have Less bone than Weight Lifters? A Vital Biomechanical View and Explanation. (1997). *Bone, 20(3),* 183-189. https://doi.org/10.1016/s8756-3282(96)00311-0

[51] Hart, N.H., Nimphius, S., Rantalainen, T., Ireland, A., Siafarikas, A., Newton, R.U. (2017). Mechanical basis of bone strength: influence of bone material, bone structure, and muscle action. *J Musculoskelet Neuronal Interact., 17(3),* 114-139. PMID: 28860414

[52] Burr, D.B., Forwood, M.R., Fyhrie, D.P., Martin, R.B., Schaffler, M.B., Turner, C.H. (2009). Bone Microdamage and Skeletal Fragility in Osteoporotic and Stress Fractures. *Journal of Bone and Mineral Research, 12(1),* 6-15. https://doi.org/10.1359/jbmr.1997.12.1.6

[53] Pellikaan, P., Giarmatzis, G., Vander Sloten, J., Verschueren, S., Jonkers, I. (2018). Ranking of osteogenic potential of physical exercises in postmenopausal women based on femoral neck strains. PLoS ONE, 13(4). https://doi.org/10.1371/journal.pone.0195463

[54] [51] Davis, I.S., Futrell, E. (2016). Gait Retraining: Altering the Fingerprint of Gait.
Phys Med Rehabil Clin N Am, 27(1), 339-355. https://doi.org/10.1016/j.pmr.2015.09.002

[55] Beck, T.J., Ruff, C.B., Shaffer, R.A., Betsinger, K., Trone, D.W., Brodine, S.K. (2000). Stress-fracture in military recruits: gender differences in muscle and bone susceptibility factors. *Bone, 27,* 437-444.

[56] Seeman, E. (2001). Sexual Dimorphism in Skeletal Size, Density, and Strength. *The Journal of Clinical Endocrinology & Metabolism, 86(10),* 4576-4584. https://doi.org/10.1210/jcem.86.10.7960

[57] Traina, F., De Clerico, M., Biondi, F., Pilla, F., Tassinari, E., Toni, A. (2009). Sex Differences in Hip Morphology: Is Stem Modularity Effective for Total Hip Replacement. *Journal of Bone and Joint Surgery, 91(6),* 121-128. https://doi.org/10.2106/JBJS.I.00533

[58] Vahdati, A., Walscharts, S., Jonkers, I., Garcia-Aznar, J.M., Vander Sloten, J., van Lenthe, G.H. (2014). Role of subject-specific musculoskeletal loading on the prediction of bone density distribution in the proximal femur, *Journal of the Mechanical Behavior of Biomedical Materials, 30*. 244-252. https://doi.org/10.1016/j.jmbbm.2013.11.015

[59] Siddiqui, J.A., Partridge, N.C. (2016). Physiological Bone Remodeling: Systemic Regulation and Growth Factor Involvement. *Physiology, 31(3),* 233-245. https://doi.org/10.1152/physiol.00061.2014

[60] O'Kane, J.W., Hutchinson, E., Atley, L.M., Eyre, D.R. (2006). Sport-related differences in biomarkers of bone resorption and cartilage degradation in endurance athletes.

[61] Wesseling, M., de Groote, F., Meyer, C., Corten, K., Simon, J., Desloovere, K., Jonkers, I. (2015). Gait Alterations to Effectively Reduce Hip Contact Forces. *Gait Alterations to Effectively Reduce Hip Contact Forces,* 1094-1102. https://doi.org/10.1002/jor.22852

[62] Crowell, H.P., Davis, I.S. (2011). Gait Retraining to Reduce Lower Extremity Loading in Runners. *Clinical Biomechanics, 26(1)*, 78-83. https://doi.org/10.1016/j.clinbiomech.2010.09.003

[63] Frankel, V.H., Burstein, A.H. (1970). Orthapaedic Biomechanics: The application of engineering to the musculoskeletal system. *Philadelphia: Lea & Febiger.*

APPENDIX A: Female Abductor Load Angle Calculation

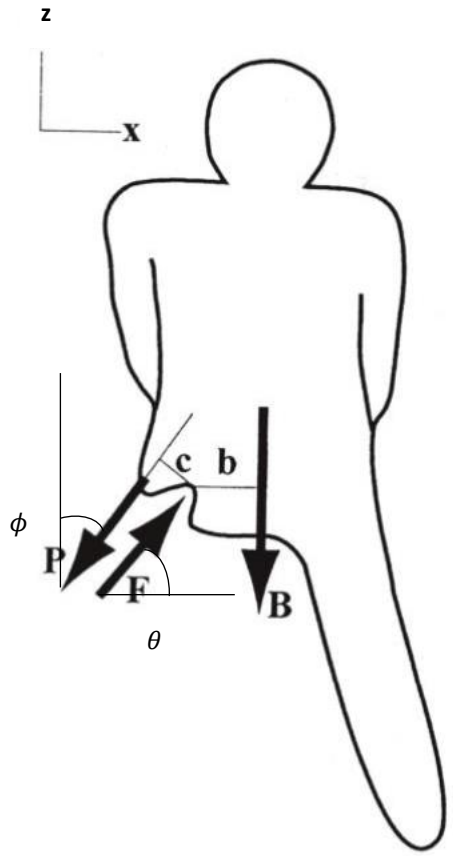

Assumptions:

- Single-leg stance phase
- B = 5/6(Body Weight)
- P = Abductor muscle force
  = Gluteus medius muscle force + Gluteus minimus muscle force
- $\theta = 22°$ for both male and female

Calculating *b* (Distance from joint center to center of gravity):

b = w/2 + r

w = Inter-hip distance between medial acetabular rims

r = Femoral head radius

Males:

w_{male} = 12.94 cm, r_{male} = 2.68 cm (From Kralj-Iglič [11])

b_{male} = 9.2 cm

Females:

w_{male} = 14.05 cm, r_{male} = 2.38 cm (From Kralj-Iglič [17])

b_{female} = 9.4 cm

Calculating *c* (Gluteal moment arm):

c = Gluteal moment arm

Assuming **c_{male} = 3.5 cm**

$c_{male} = 1.2 * c_{female}$ (From Woyski et al. [36])

c_{female} = 2.9 cm

The b/c ratio is typically between 2 – 3.5 (From Frankel and Burstein [63]):

b/c_{male} = 9.2 cm/ 3.5 cm = 2.6

b/c_{female} = 9.4 cm/2.9 cm = 3.2

Therefore, these gluteal moment arms are appropriate for this model.

Solving for P_{xz} (Magnitude of abductor muscle force in x-z plane):

From male baseline model with 725 N body weight:

P_x = (gluteus medius)$_x$ + (gluteus minimus)$_x$ = 304 N + 152 N = 456 N

P_z = (gluteus medius)$_z$ + (gluteus minimus)$_z$ = 486 N + 239 N = 725 N

$P_{xz} = \sqrt{P_x^2 + P_z^2}$ = **857 N**

For female baseline model with 556 N body weight:

P_x = (gluteus medius)$_x$ + (gluteus minimus)$_x$ = 233 N + 116 N = 349 N

P_z = (gluteus medius)$_z$ + (gluteus minimus)$_z$ = 373 N + 183 N = 556 N

$P_{xz} = \sqrt{P_x^2 + P_z^2}$ = **657 N**

Solving for F_{xz} (Magnitude of joint contact force in x-z plane):

From male baseline model with 725 N body weight:

(Constants from Deuel [28])

F_x = 0.90BW = 653 N

F_z = 2.27BW = 1646 N

$F_{xz} = \sqrt{F_x^2 + F_z^2}$ = **1810 N**

For female baseline model with 556 N body weight:

F_x = 0.90BW = 500 N

F_z = 2.27BW = 1262 N

$F_{xz} = \sqrt{F_x^2 + F_z^2}$ = **1357 N**

Static Equilibrium Equations:

$\Sigma M_O = 0 = -B(b) + P(c)$ (Equation 1)

$\Sigma F_x = 0 = F_x - P_x$ (Equation 2)

$F_x = P sin\phi$

$P = F_x / sin\phi$

Substitute Equation 2 into Equation 1, and solve for ϕ:

$\boldsymbol{\phi = \sin^{-1}(\frac{F_x}{B} * \frac{c}{b})}$

Solve for male and female abductor x-z load angles:

$$\phi_{male} = \sin^{-1}\left(\frac{F_x}{B} * \frac{c}{b}\right) = \sin^{-1}\left(\frac{653\ N}{604\ N} * \frac{0.035\ m}{0.092\ m}\right) = \mathbf{24.2°}$$

$$\phi_{female} = \sin^{-1}\left(\frac{F_x}{B} * \frac{c}{b}\right) = \sin^{-1}\left(\frac{500\ N}{463\ N} * \frac{0.029\ m}{0.094\ m}\right) = \mathbf{19.4°}$$

Use angles to determine female abductor x-z load components:

Gluteus medius magnitude in the x-z direction:

$F_{xz} = \sqrt{F_x^2 + F_z^2}$ = 440 N (At baseline heel-strike)

x-component magnitude:

$F_{x_{female}} = F_{xz} sin\phi = 440N * \sin(19.4°) = \mathbf{230\ N}$

z-component magnitude:

$F_{z_{female}} = F_{xz} cos\phi = 440N * \cos(19.4°) = \mathbf{375\ N}$

Gluteus minimus magnitude in the x-z direction:

$F_{xz} = \sqrt{F_x^2 + F_z^2}$ = 217 N (At baseline heel-strike)

x-component magnitude:

$F_{x_{female}} = F_{xz} sin\phi = 217N * \sin(19.4°) = \mathbf{114\ N}$

z-component magnitude:

$F_{z_{female}} = F_{xz} cos\phi = 217N * \cos(19.4°) = \mathbf{185\ N}$

APPENDIX B: Female Hip Joint Stress Calculation

Assumptions:

Male bodyweight (BW_{male}) = 725 N

Female bodyweight (BW_{female}) = 556 N

Male Hip Joint Stress:

Stress/BW = 3.214 kPa/N (From Iglic et al. [9])

For a 725 N male:

725 N * 3.214 kPa/N = **2.33 MPa**

Female Hip Joint Stress:

Stress/ BW = 4.045 kPa/N (From Iglic et al. [9])

For a 556 N female:

556 N * 4.045 kPa/N = **2.25 Mpa**

Male Hip Joint Stress/ Female Hip Joint Stress = 2.33/2.25 = 1.04

For a 725 N male and 556 N female:

Female Hip Joint Stress = 0.96(Male Hip Joint Stress)

FE-Model loads:

Hip Joint Force magnitude = 250% BW

Joint pressure area = 33 mm^2

Hip Joint Stress [MPa] = 2.50*(Bodyweight [N])/33mm^2

Male Hip Joint Stress = 2.50(725 N)/33mm^2 = **3.33 MPa**

Female Hip Joint Stress = 0.96(3.33 MPa) = **3.20 MPa**

Appendix C : Marathon Training Schedule

	MILES							
Week	**Mon**	**Tue**	**Wed**	**Thu**	**Fri**	**Sat**	**Sun**	**Total**
1	5	6	0	5	4	10	0	30
2	5	7	0	5	4	12	0	33
3	5	8	0	6	3	14	0	36
4	6	5	0	6	5	10	0	32
5	6	7	0	6	5	14	0	38
6	6	7	0	6	4	17	0	39
7	4	8	0	7	4	18	0	41
8	7	5	0	8	5	12	0	37
9	6	7	0	6	5	13	0	37
10	5	8	0	6	5	18	0	42
11	6	5	0	10	4	20	0	45
12	7	8	0	6	5	15	0	41
13	5	5	0	6	4	18	0	38
14	5	9	0	6	5	15	0	40
15	4	5	0	5	4	10	0	28
16	3	5	0	4	0	3	26	41

(Based on Runner's World Intermediate Marathon Training Schedule by Hobson, B. [42])

APPENDIX D: Femur Contour Plots

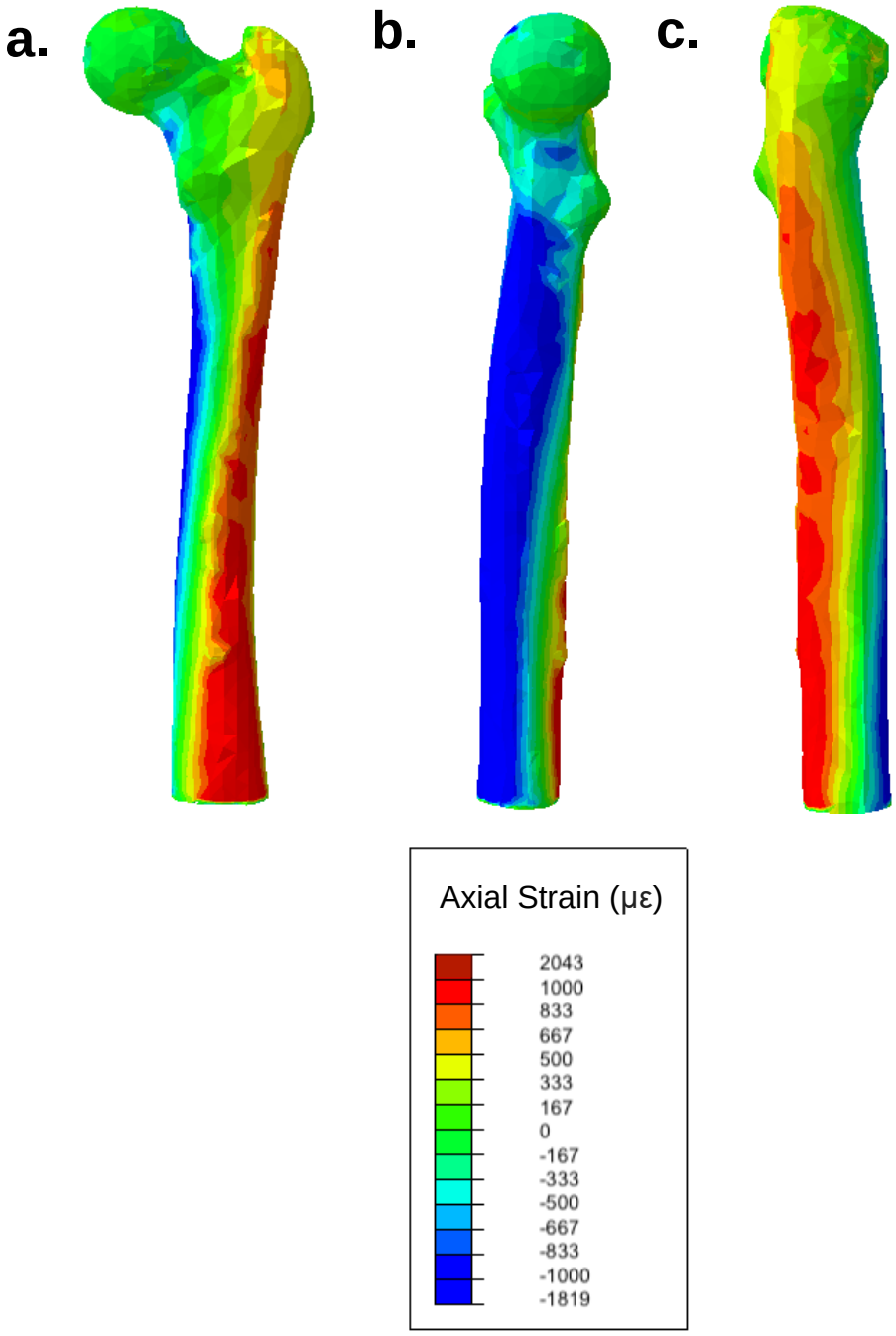

Figure D1. Predicted femoral axial strain for male baseline.

a) Anterior View, b) Medial View, c) Lateral View

(Strain is measured in microstrain, Microstrain = Strain X 10^6. Positive strain is tensile and negative strain is compressive.)

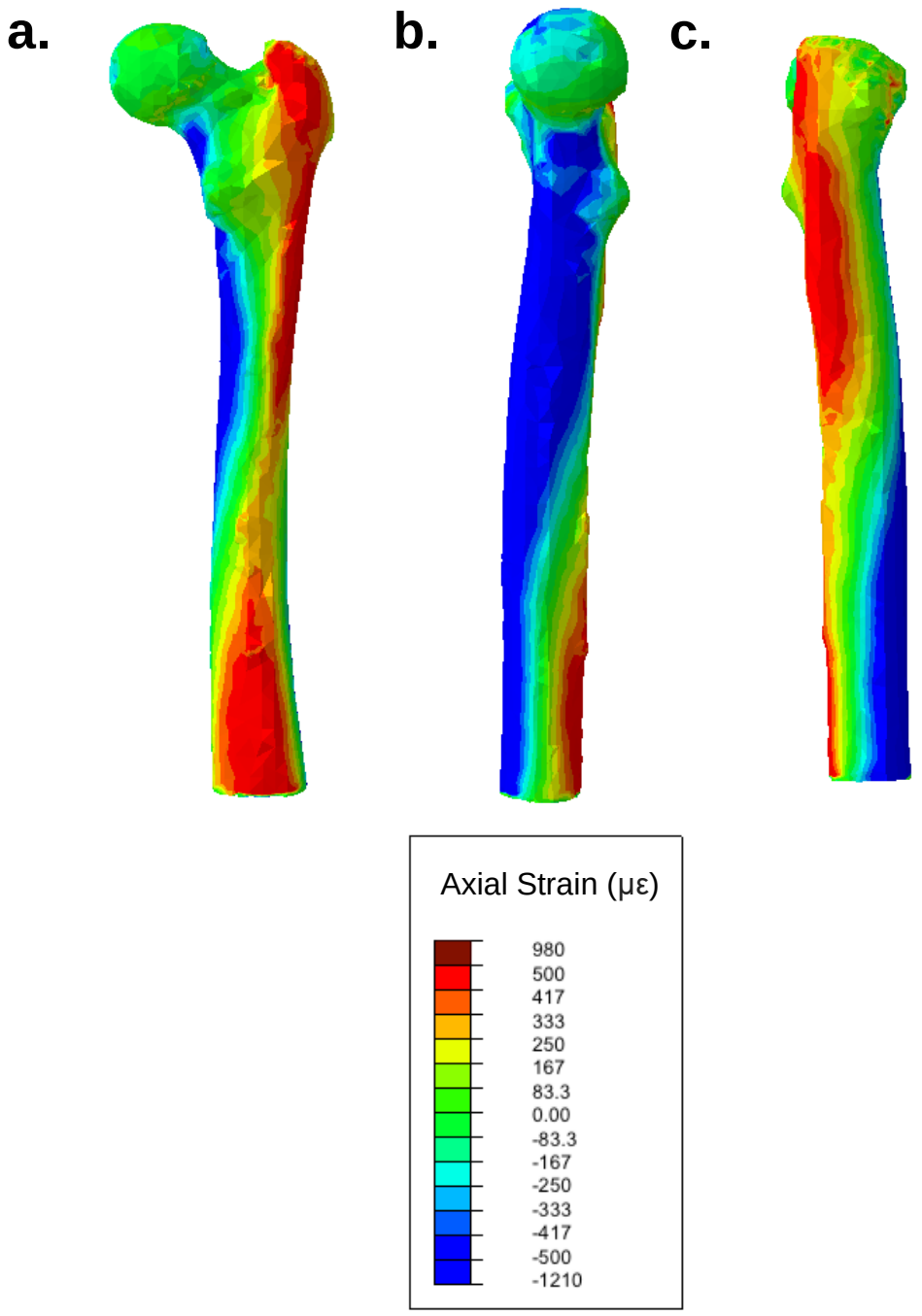

Figure D2. Predicted femoral axial strain for female baseline.

a) Anterior View, b) Medial View, c) Lateral View

(Strain is measured in microstrain, Microstrain = Strain X 10^6. Positive strain is tensile and negative strain is compressive.)

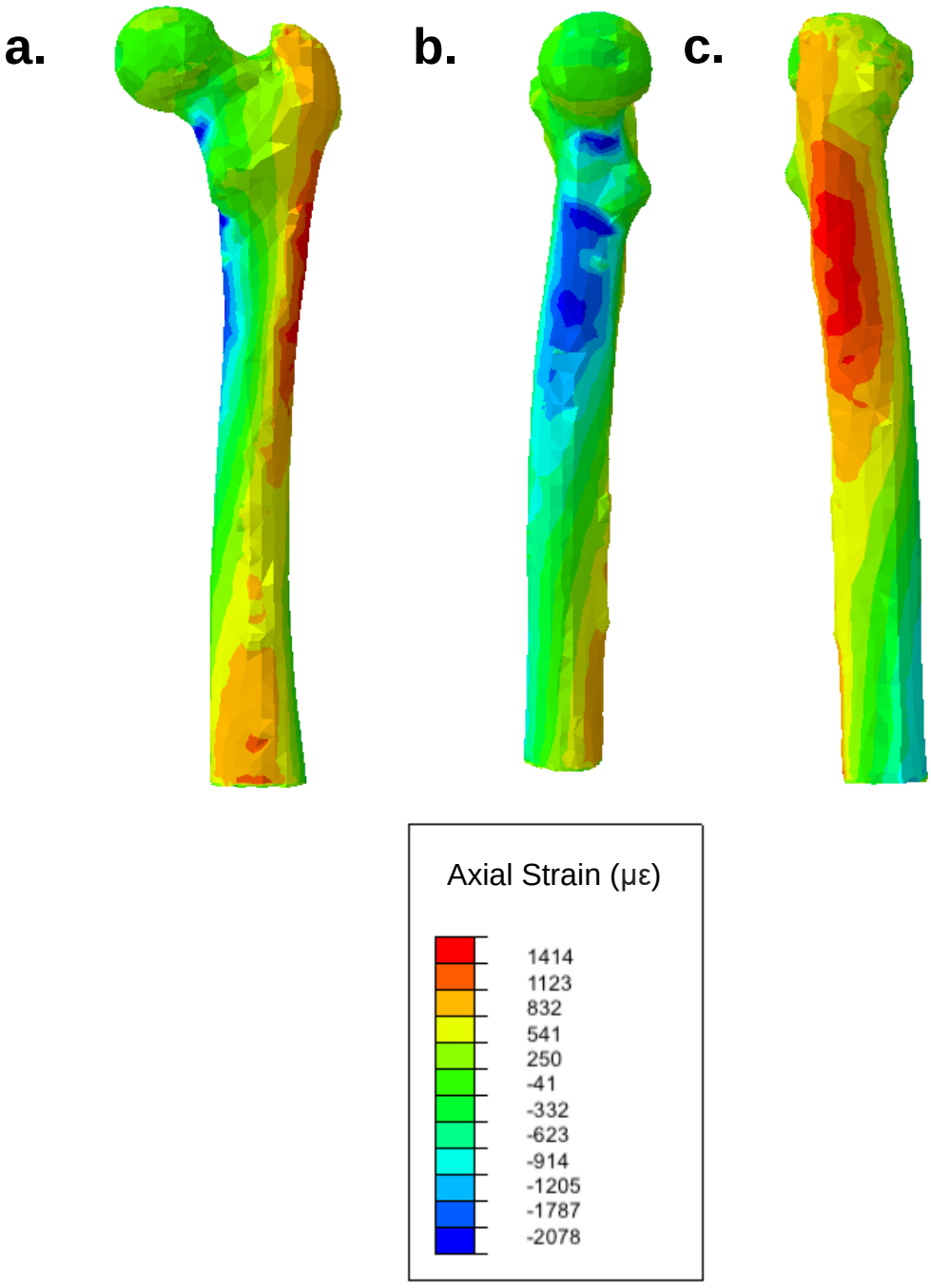

Figure D3. Predicted femoral axial strain for male following marathon training.

a) Anterior View, b) Medial View, c) Lateral View

(Strain is measured in microstrain, Microstrain = Strain X 10^6. Positive strain is tensile and negative strain is compressive.)

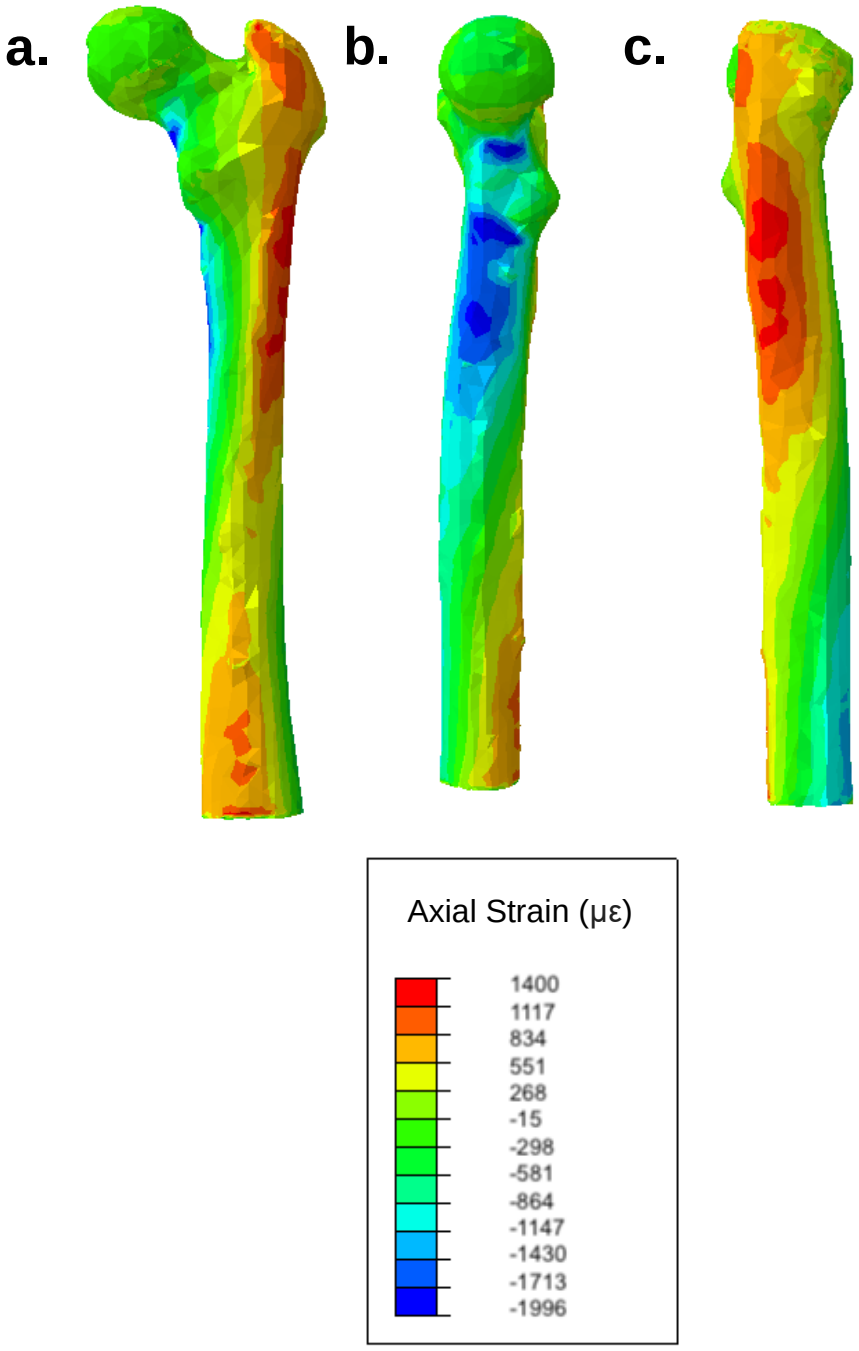

a) **Figure D4.** Predicted femoral axial strain for female following marathon training.

a) Anterior View, b) Medial View, c) Lateral View

(Strain is measured in microstrain, Microstrain = Strain X 10^6. Positive strain is tensile and negative strain is compressive.)

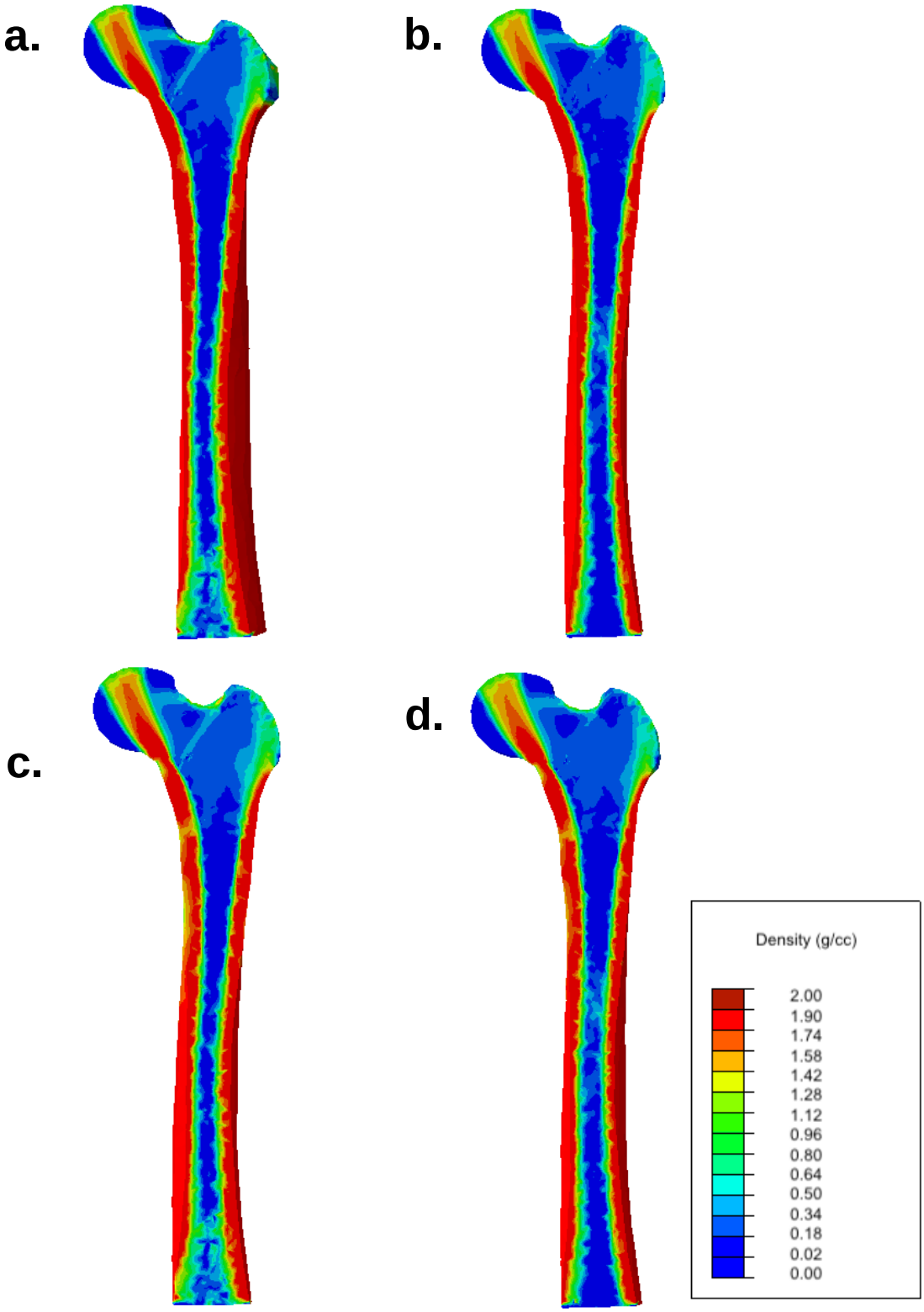

Figure D5. Predicted femoral bone mineral density for a) male baseline, b) female baseline, c) male following marathon training, d) female following marathon training

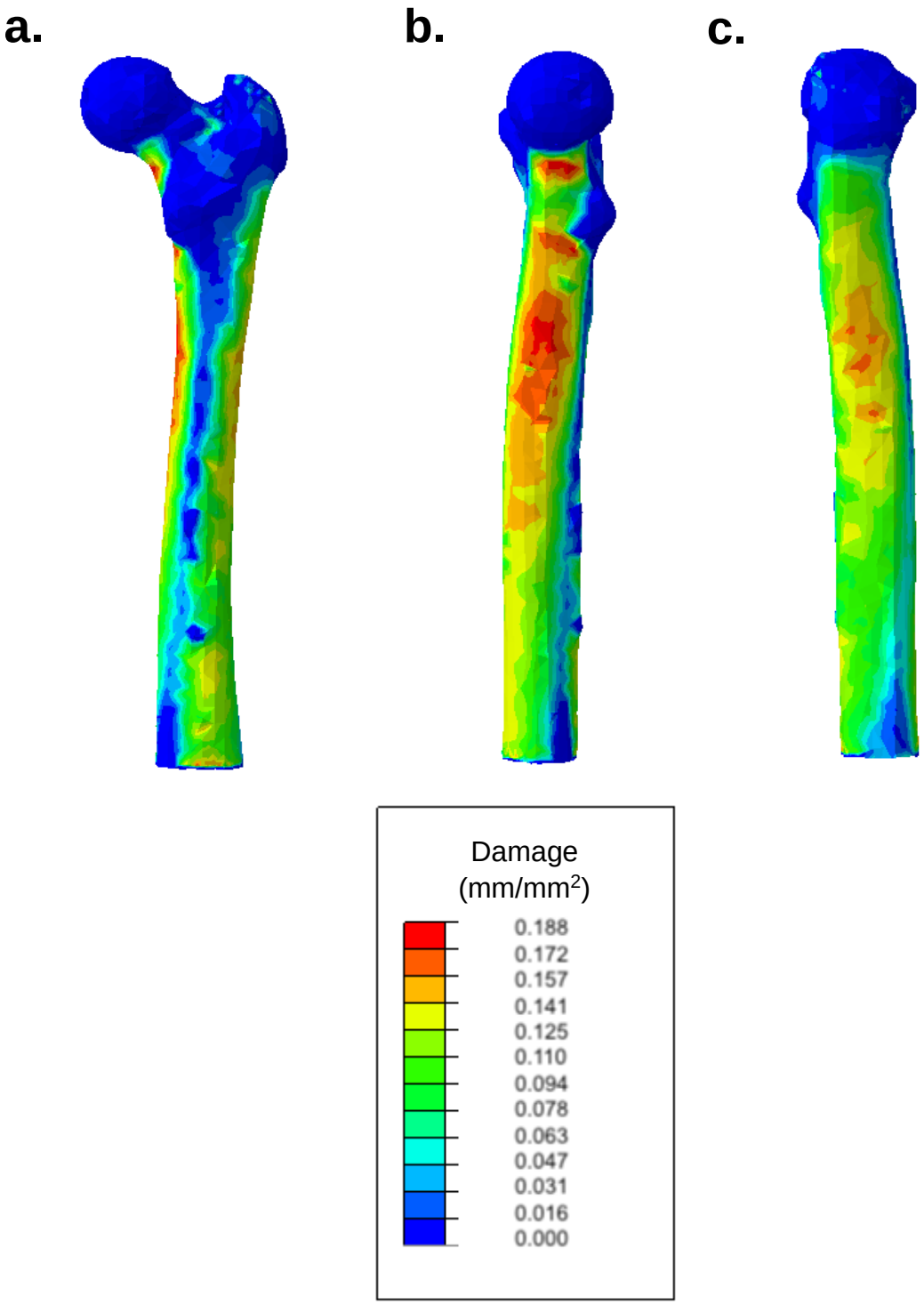

Figure D6. Predicted femoral damage for male baseline

a) Anterior View, b) Medial View, c) Lateral View

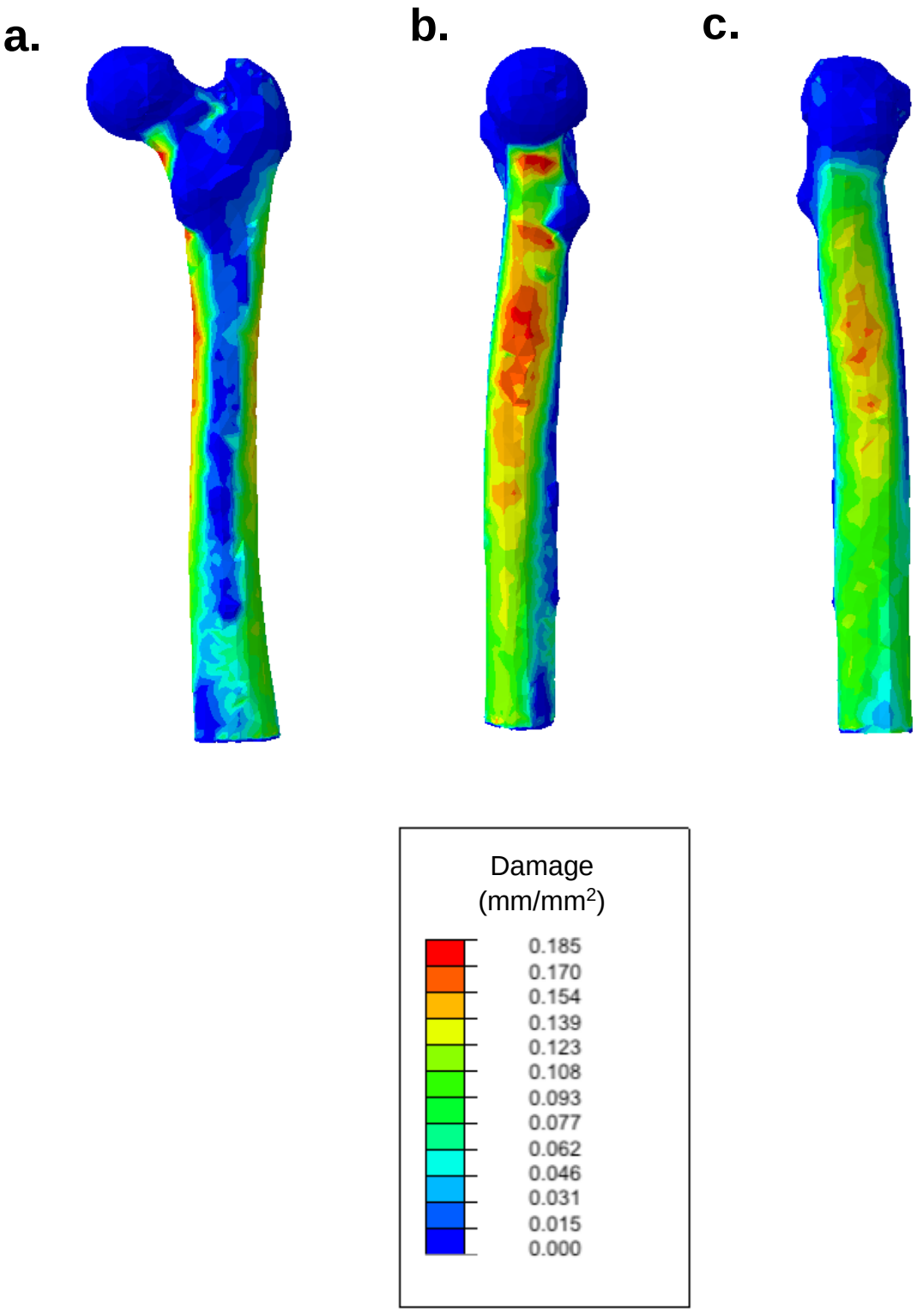

Figure D7. Predicted femoral damage for female baseline

a) Anterior View, b) Medial View, c) Lateral View

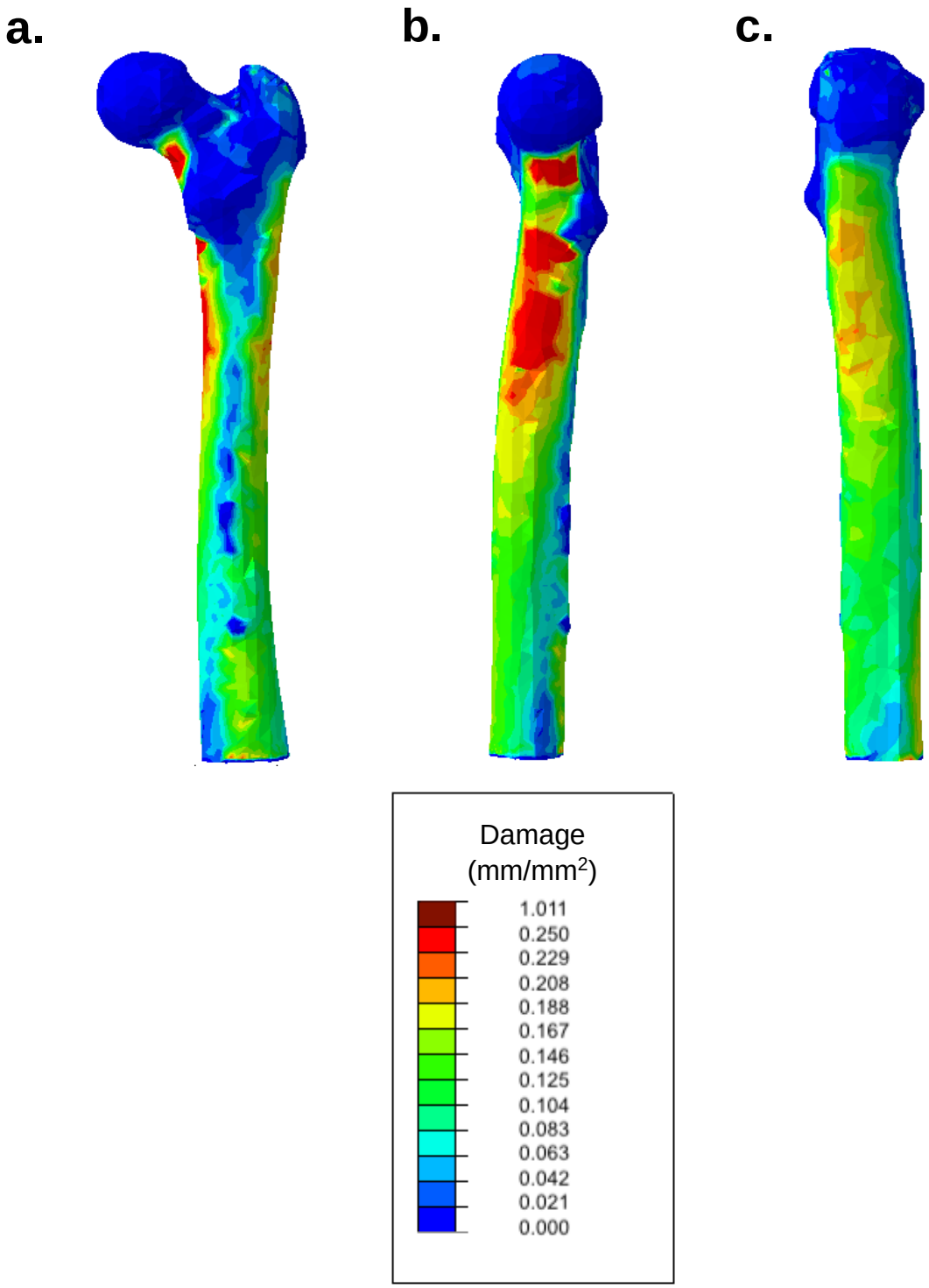

Figure D8. Predicted femoral damage for male following marathon training a) Anterior View, b) Medial View, c) Lateral View

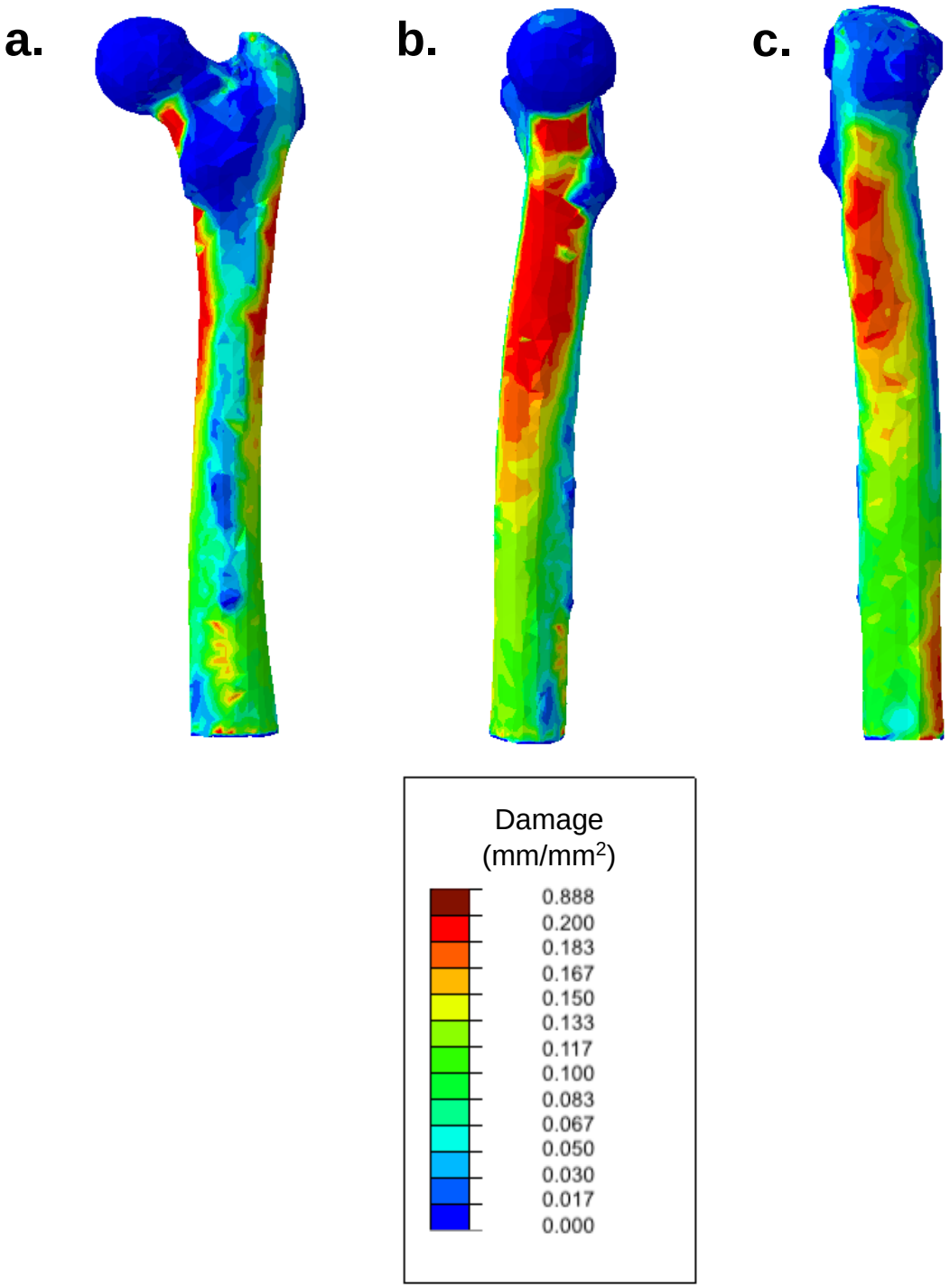

Figure D9. Predicted femoral damage for female following marathon training

a) Anterior View, b) Medial View, c) Lateral View

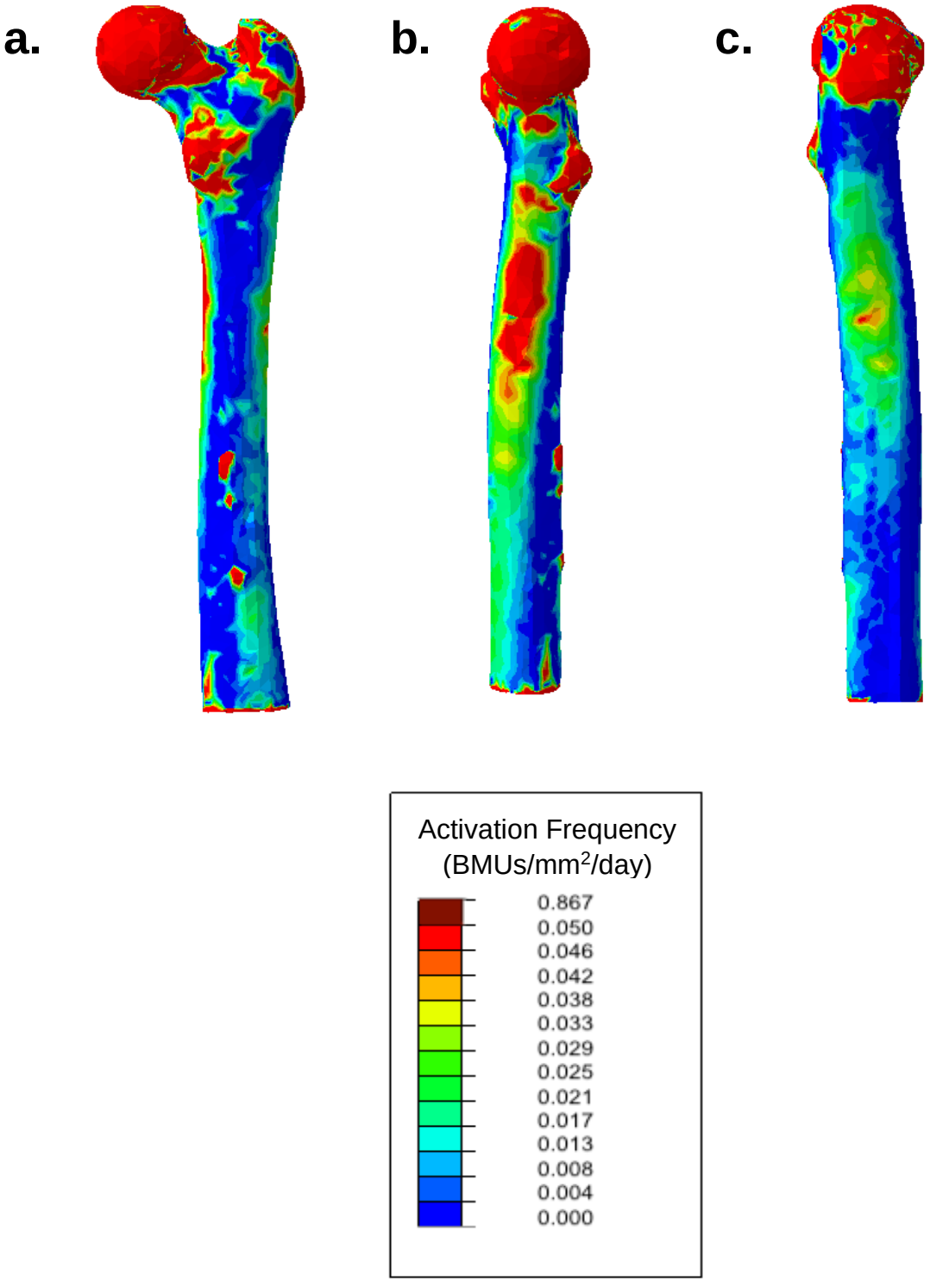

Figure D10. Predicted femoral activation frequency for male baseline

a) Anterior View, b) Medial View, c) Lateral View

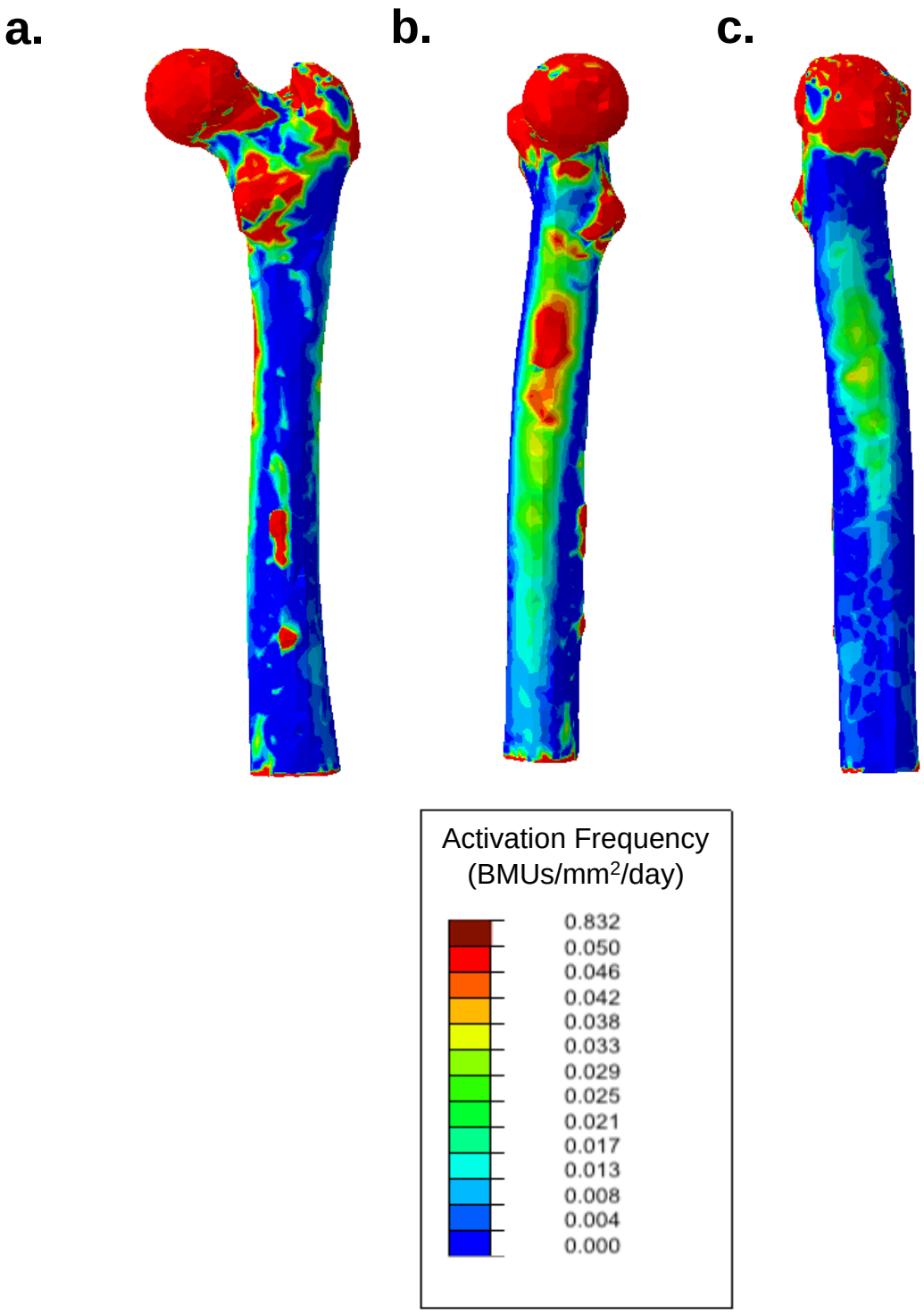

Figure D11. Predicted femoral activation frequency for female baseline a) Anterior View, b) Medial View, c) Lateral View

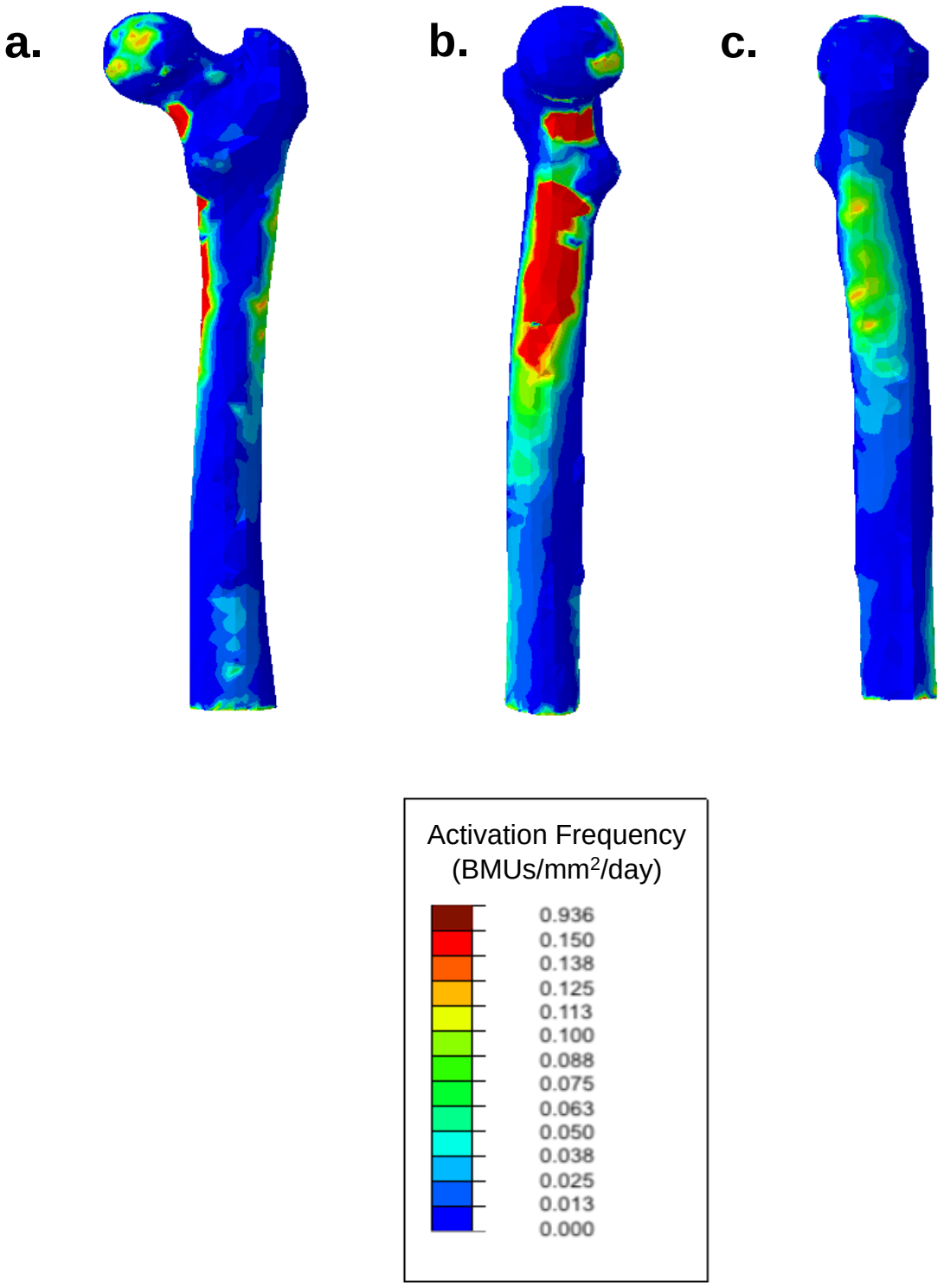

Figure D12. Predicted femoral activation frequency for male following marathon training

a) Anterior View, b) Medial View, c) Lateral View

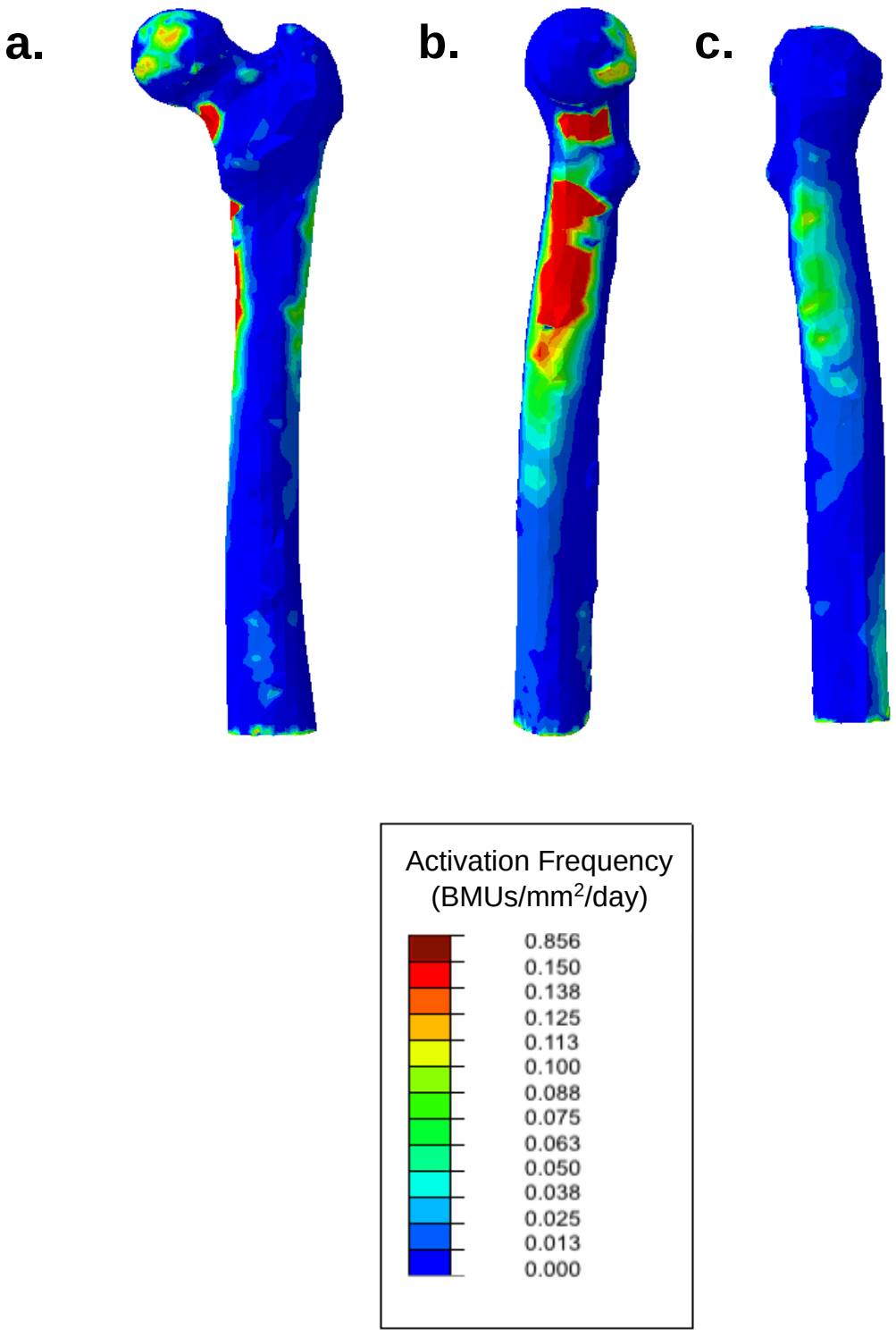

Figure D13. Predicted femoral activation frequency for female following marathon training

a) Anterior View, b) Medial View, c) Lateral View